THE TOXICITY OF SILVER NANOPARTICLES

UNIVERSITY *of the*
WESTERN CAPE

By

Khothatso Patricia Motsoeneng

A mini thesis submitted in partial fulfilment of the requirements for the degree of Masters of Science in Nanoscience, University of the Western Cape

Supervisor: Prof Edmund Pool (Medical Bioscience Department)
Co-Supervisor: Prof Leslie Petrik (Chemistry Department)

July 2015

Abstract

Unavailability and contamination of available water resources are major factors contributing to adverse health conditions worldwide. AgNPs present a potential strategy for water purification; however, their ability to accumulate in organs such as the kidneys, lungs and spleen is a possible source of toxicity. This study investigates the toxicity of AgNPs to *Saccharomyces cerevisiae (S. cerevisiae). S. cerevisiae* is an excellent model organism for assessing toxic compounds that affect eukaryotic organisms due to their ease of cultivation. AgNPs were prepared by photo-reduction of silver nitrate with OSRAM Vitalux lamp (300 W and 230 V) in the presence of stabilizing agents such as polyvinylpyrrolidone and citric acid, yielding AgNPs. The effects of varying the concentration of the stabilizing agent, time of exposure to the light source, and pH were investigated. The formation of AgNPs was analysed by ultra-violet spectroscopy (UV-Vis) and transmission electron microscope techniques. The results showed that the AgNPs absorbed ultra-violet radiation between 400 and 500 nm and TEM images showed the particles to be both spherical and needle-like in shape. The shapes of the AgNPs were largely dependent on the synthesis method applied. The toxicity of AgNPs was assessed using metabolic activity of yeast cells as biomarker and monitored with of the chromogenic assay, XTT. *S. cerevisiae* was introduced into different concentrations of AgNPs and incubated at 37^{o}C for 72 h. After the incubation, XTT assay was performed to assess the cell viability. The XTT results showed that high concentration of AgNPs (100 µg/mL) inhibited the growth of *S. cerevisiae*. The synthesis of AgNPs and the assessment of their toxicity on *S. cerevisiae* was thus undertaken and established in this work.

Keywords

Silver nanoparticles (AgNPs)

Water purification

Photoreduction

Citric acid

Toxicity

S. cerevisiae

Chromogenic assay

DECLARATION

I declare that "*The toxicity of silver nanoparticles*" is my own work that has not been submitted for any other degree or examination in any other university and that all the sources I have used or quoted have been indicated and acknowledged by complete references.

Khothatso Patricia Motsoeneng July 2015

Signed.....

ACKNOWLEDGEMENTS

Firstly, I would like to give thanks to God Almighty for giving me strength and keeping me thus far.

Secondly, I would like to acknowledge my supervisor and co-supervisor: Prof Edmund Pool and Prof Leslie Petrik, for their support and readiness to impart skills and knowledge. They encouraged and challenged me to perform to the best of my potential and I am grateful for that.

Thirdly, I render many thanks to Mr Valentine Anye (University of Pretoria), for editing and proofreading this work. Your effort is highly appreciated. To my colleagues Roland, Missengue, Jimoh and everyone from Environmental and Nanoscience Research group, I say thank you for your many suggestions and inputs into this research endeavour.

I would also like to appreciate the Department of Science and Technology (DST) for funding my project and the Departments of Medical Bioscience and Chemistry at UWC, together with the University of Cape Town (UCT) for allowing me to use their equipment and resources for this work.

Fourthly, I would love to thank my mom, Makeiso Motsoeneng, for her encouraging words, prayers and support; you are the best mom ever. Special thanks to my brothers and sisters Tebello, Teboho, Keiso, Rapelang, Edisang and Thabisang; your support is highly appreciated.

Finally yet importantly, I would like to appreciate the support of my friends: Lindi, Mzwandile and Busiswa for the encouragement and support they gave me during this work.

TABLE OF CONTENTS

LIST OF TABLES

LIST OF FIGURES

LIST OF ABBREVIATIONS

$AgNO_3$	Silver nitrate
AgNPs	Silver nanoparticles
EtOH	Ethanol
GSH	Glutathione S-transferase
HR-TEM	High Resolution-Transmission Electron Microscope
ID	Identity
MEB	Malt extract broth
NH_4OH	Ammonium hydroxide
OD	Optical density
PBS	Potassium buffered saline
PDA	Potato extract broth
PVP	Polyvinylpyrrolidone
ROS	Reaction oxidative species
SDS	Sodium dodecyl sulfate
UV-Vis	Ultra-violet
XTT	2,3-Bis(2-methyloxy-4-nitro-5-sulfophenyl)-5-[(phenylamino) Carbonyl]-2H-tetrazolium hydroxide

CHAPTER 1

This chapter gives a short background about water scarcity worldwide and also highlights the improvements to be made to overcome this challenge. Furthermore, the importance of this study, the problem statement, research questions, research approach with its scope, delimitations, aims and objectives are covered in this chapter. The chapter ends with a brief outline of the structure of this thesis.

1.1 Background

Unavailability and contamination of available water is a major health challenge globally, and in developing countries particularly (WHO, 2008). This challenge results in disease and economic dilemmas especially in marginalized communities. With extended droughts, increasing populations and competing demand from various users, the need of clean water supply has become a major necessity for governments worldwide (Savage and Diallo, 2005). Water that does not contain toxic pollutants is essential for human health. The prevalence of most enteric diseases is due to bacterial contamination of drinking water. According to the World Health Organization (WHO), approximately 1.8 million deaths and 61.9 million disability adjusted life years (DALY'S) globally are due to unsafe water, sanitation and poor hygiene. It has been estimated that 99.8% of such deaths mainly occur in developing countries with children ranking (90%) as the first victims. Contamination of ground and surface water with pathogenic bacteria such as *Escherichia coli* O157:H7, *Salmonella typhimurium*, *Shigella dysenteriae* and *Vibrio cholera* are the major causes of diarrheal and gastrointestinal infections (Savage and Diallo, 2005). This is an indication that safe drinking water plays a huge role in human health and well-being. Infections from water are generally classified into four categories namely: water borne, water washed, water based and water

related diseases. The first three classes are mostly associated with the lack of good water supplies.

Water borne diseases are diseases resulting from the ingestion of water contaminated with pathogens. These diseases include most enteric and diarrheal diseases caused by viruses and bacteria in water. Water washed diseases result from inadequate supply of clean water for personal hygiene and washing (Hunter *et al.,* 2000). Water based diseases are obtained from hosts that live in water. Humans are likely to contract these kinds of diseases from ingestion or walking in contaminated water. Water related disease includes diseases distributed by insects that breed or feed near contaminated water such as malaria, dengue fever and onchocerciasis (Hunter *et al.,* 2000).

Though several systems and techniques have been developed for wastewater treatment, these systems still do not remove all contaminants in water. The removal or inactivation of pathogenic bacteria is often the last step in wastewater treatment systems (Tiwari *et al.*, 2008). Some techniques used for wastewater treatment involve the use of chemicals and physical agents such as chlorine and its derivatives, ultra-violet light, boiling, low frequency ultrasonic irradiation, distillation, water sedimentation and reverse osmosis. Halogens such as chlorine and bromine are used as antibacterial agents. The direct use of these halogens, however, causes problems due to the high toxicity and vapour pressure of these chemicals in pure form (Tiwari*, et al.*, 2008). Another chemical compound, ammonium (NH_4^+), a common cation in water has been shown to have serious adverse effects on both human and animal health. This compound is found in wastewater and small proportions of it manage to be oxidized in water during conventional treatment in treatment plants. Coupled with the decomposition of organic matter in water, the presence of oxidized NH_4^+, reduces the amount

of oxygen that can be dissolved by water, posing a potential detrimental consequences to aerobic biota.

Ongoing research is attempting to use AgNPs for water purification to provide safe drinking water. AgNPs are simple and inexpensive disinfection systems, which could provide safe drinking water for millions of people in areas where there are shortages of clean water (Dankovich and Gray, 2011). Several clay pot-based, water treatment systems and devices are currently being used internationally by small rural areas, which lack safe water. Although South Africa has done some exploratory work that relates to the use of these clay pots for hygiene purpose, little on evaluation of the safety of these units or improving them has been accomplished. These units can be a great empowerment tool for rural communities lacking water service. Clay pots have been used in countries such as Nicaragua and Cambodia for some time but silver, used as the antimicrobial agent is simply painted onto the surface. The incorporation of silver throughout the pot may increase water treatment efficiency (Vinka *et al.,* 2008).

1.2 Aim and objectives

The aim of this study was to investigate the toxicity of AgNPs on yeast cell *(S. cerevisiae*).

The objectives of the study are as follows:

- To synthesize AgNPs from silver nitrate ($AgNO_3$) using photolight as a reducing agent.
- To characterize the synthesized AgNPs using Ultra-Violet spectroscopy (UV-Vis) and Transmission Electron Microscope (TEM).
- To examine the toxicity of silver to yeast cells and by observing the cell viability

1.3 Research questions

- Does photoreduction method produce different shapes of silver nanoparticles?
- Which stabilizing agent (PVP or citric acid) produce small sizes of silver nanoparticles?
- What effects do AgNPs have on the *S. cerevisiae* cell?
- Is *S. cerevisiae* a good indicator for toxicity of AgNPs?

1.4 Research approach

The schematic flow diagram (Figure 1) presents the research approach used to synthesize AgNPs and to examine the toxicity of the synthesized AgNPs.

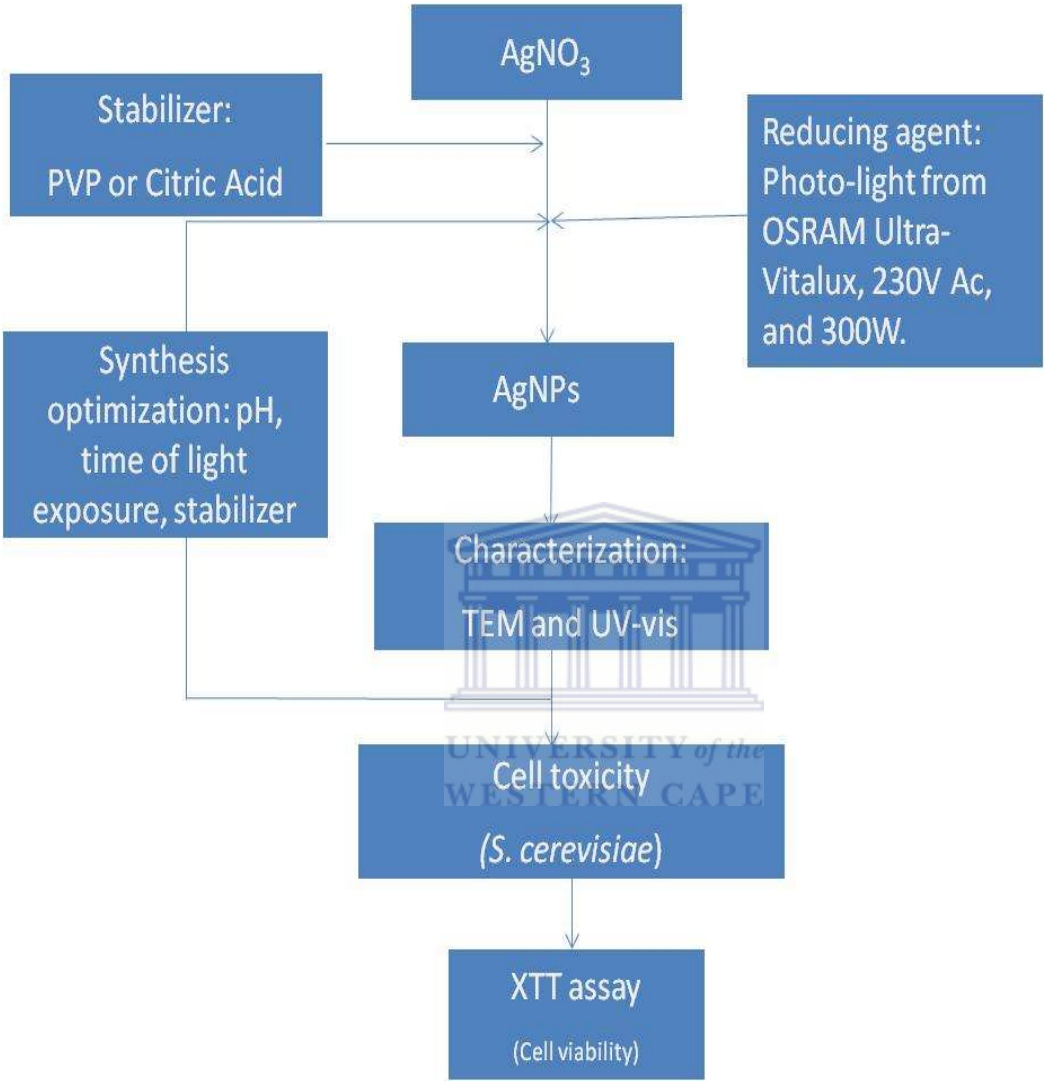

Figure 1: Schematic flow diagram for synthesis of AgNPs and determining their toxicity on the yeast cell.

AgNPs were synthesised by reducing silver nitrate ($AgNO_3$) with photolight (OSRAM ultra-vitalux, 230V Ac, 300W) in the presence of PVP or citric acid as stabilizer. The obtained AgNPs were characterized by UV-Vis and TEM techniques. Optimization of nanoparticles size was achieved by varying parameters such as molar ratio, time of light exposure and pH. The obtained AgNPs were used to investigate their toxicity on *S. cerevisiae.* Cell proliferation was investigated using XTT assays.

1.5 Scope and delimitations

This study focused on the synthesis of AgNPs from silver nitrate ($AgNO_3$) using a photolight source (OSRAM ultra-vitalux, 230V Ac, 300W) as reducing agent. UV-vis and TEM were used to characterize the synthesized AgNPs. AgNPs purification could not be done and extensive characterization methods, including XDR, FTIR and SEM could not be used due to time constraints. The toxicity of these nanoparticles was investigated on *S. cerevisiae,* a model organism for assessing toxic compounds affecting eukaryotic cells. Owing to the time, financial and ethical restrictions, animal models (such as rats) could not be used for this study. The effect of AgNPs on yeast cells was investigated in this study using XTT assay and toxicity of stabilizing agents such as PVP and citric acid could not be investigated due to time limitation. It is important to note here that, this work was a mini thesis, with just a year allocated for research and writing following an intensive year of purely course work. Hence, the time limitation mentioned in this section.

1.6 Thesis structure

Chapter-2 Literature Review and Theoretical framework

Chapter 2 lays out the theoretical framework of this research and covers general information on the toxicity of AgNPs to microbes. The chapter also gives insights into the techniques that have been applied in characterization of synthesized nanoparticles.

Chapter-3 Problem statement

Chapter3 presents the problems of water scarcity and sanitation in rural areas. It also highlights the problems of current techniques used to purify water and suggest a way forward.

Chapter-4 Preparation and characterization of AgNPs

Chapter 4 describes the methodology used in this work to synthesize nanoparticles and characterize them. TEM and UV-Vis were used to analyse the synthesized AgNPs. The results of the characterized AgNPs are also presented and discussed in this chapter.

Chapter-5 Toxicity testing of AgNPs

Chapter 5 outlines and describes the methodology used to assess the toxicity of AgNPs. An XTT assay was used to assess the proliferation of *S. cerevisiae* cells. Results are presented and discussed.

Chapter-6 Conclusion and Recommendations

This chapter summarized the whole study and highlights the achievements and contributions of the study. The chapter proposes away forward and aspects for further research.

CHAPTER 2: LITERATURE REVIEW

2.1 Introduction

This chapter presents the literature review of this study. It will be divided into two sections. The first section will review silver ions and various methods to synthesize AgNPs and techniques used to characterize them. The second section reviews growth of *S. cerevisiae*, toxicity of AgNPs and the colorimetric assays used to examine cell proliferation and cell viability.

2.2 Silver

Silver is a naturally occurring metal, appearing most often as a mineral and is positioned as the 47th element on the periodic table with an atomic weight of 107.8. Silver has two natural isotopes Ag 106.90 and Ag 108.90 with respective abundances of 52 and 48%. This metal has been used in a variety of applications, due to its high electric and thermal conductivity (Nordberg and Gerhardsson, 1988). Ancient civilizations used silver in medicine, food containers, plates, eating utensils, cups, money, jewellery, clothes and for water disinfection.

Naturally, silver possesses antimicrobial activity towards many pathogens including bacteria, fungi, yeasts and viruses (Zhang and Sun, 2007). The silver salts like silver nitrate, have been used to treat mental illness, gastroenteritis, nicotine addiction and infectious diseases such as gonorrhea and syphilis (Gulbranson *et al.,* 2000). Recently, silver-coated catheters are being used to stop infections (Samuel and Guggenbichler, 2004). In order to protect humans from food poisoning, AgNPs are now being put in tabletops, cutting boards, surface disinfectants and refrigerators. However, ecologists have warned that the widespread use of this powerful antimicrobial agent could have a negative impact for bacteria in natural ecosystems if released in waste streams. There is now growing evidence that as the silver metal is toxic to

bacteria, so are AgNPs toxic to mammalian cells (Braydich-Stolle *et al.,* 2005). In addition, AgNPs have been shown to damage liver, brain and stem cells in animal models. The over-exposure of colloidal or silver salt deposits under the skin causes skin disease such as argyria or argyrosis. Argyrosis is described as a pathologic bluish-black pigment in a tissue, which results from the deposition of an insoluble albuminate of silver (Panyala *et al.,* 2008). Silver in its bulk form, is extremely toxic to fish (Hogstrand and Wood, 1996), algae, fungi, some plants, crustaceans and bacteria such as the nitrogen fixing heterotrophic and soil forming chemolithotrophic bacteria (Eisler, 1996).

Factors such as solubility and binding specificity to a biological site influence the toxicity of silver metal. The toxic effect of metals is defined as any functional or morphological change in the body caused by consumption, injection, inhalation or absorbed drug, chemical or biological agent containing silver. Silver occurs in various forms that can affect both the environment and living things. These forms include metallic silver, silver complexes, silver salts and colloidal silver. Metallic silver dissolves in acids and forms compounds like silver nitrate (Panyala *et al.,* 2008). Aqueous solutions of silver nitrate comprises silver in the form of hydrated silver cations. Silver cations form complexes with different organic ligands and even if these cations are still present in the molecule, the charge of the complex can still be neutral. Additionally, highly stable complex forms of silver do not dissociate in solutions or liquids (Panyala *et al.,* 2008).

2.2.1 Nanoparticles

Nanoparticles are particles that have at least one dimension with a size ranging between 1 to 100 nm. They can exist in single, aggregated or agglomerated fused forms of spherical, tubular or irregular shape. The common types of nanoparticles are dendrimers, nanotubes,

quantum dots and fullerenes. Products with engineered nanoparticles have been in markets for decades now, and keep increasing as years go by. Nanoparticles are now being used for the manufacture of analytical tools for life sciences and biotechnology (Cui *et al*., 2001). Additionally, nanoparticles are applied in ultra-sensitive molecular sensing, diagnostic imaging, agents of photodynamic, wound dressings, dental-bonding agents, clothing and electronics. Despite their widespread applications, little is documented on the effects of nanoparticles on human health and the environment (Teodoro *et al.,* 2011). This calls for deliberate investigation of the toxicity of these particles on human and environmental health to be undertaken.

2.2.1.1 Silver nanoparticles

AgNPs are nanoparticles consisting of about 20 to 15,000 silver atoms. These particles occur in various shapes; spheres, rods and cubes, and sizes, but generally are smaller than 100 nm. AgNPs can also be produced as tubes, multifacets, wires and cubes. At the nano-scale, AgNPs have better physiochemical properties and greater biological activities compared to the regular bulk metal. This is as a result of the higher surface area per mass, permitting a larger amount of surface atoms to interact with the surroundings (Wijnhoven *et al.,* 2009). Nowadays, AgNPs are being used in an increasing number of consumer and medical products (Table 1) (Panyala *et al.,* 2008).

Table 1: Product categories with examples of products containing silver nanoparticles. The values between the brackets indicate the number of sub-categories (Panyala *et al.*, 2008).

Categories	Subcategories	Examples
Personal care and cosmetics (30)	Skin care (14)	(Body) cream, hand sanitizer, hair care products, beauty soap, face masks
	Oral hygiene (6)	Tooth brush, teeth cleaner, toothpaste
	Hair care (3)	Hair brush, hair masks
	Cleaning (2)	Elimination wipes and spray
	Coating (2)	Make-up instrument, watch chain
	Baby care (2)	Pacifier, teeth developer
	Over the counter health products (1)	Foam condom
Textile and shoes (34)	Clothing (28)	Fabrics and fibers, socks, shirts, caps, jackets, gloves, underwear
	Other textiles (2)	Sheets, towels, shoe care, sleeves and braces
	Toys	Plush toys
Electronics (29)	Personal care (13)	Hair dryers, wavers, ions, shavers
	Household appliances (8)	Refrigerators, washing machines
	Computer hardware (6)	Notebooks, (laser) mouse, keyboards
	Mobile devices (2)	Mobile phones
Household products/home improvement (19)	Cleaning (9)	Cleaning products for bathroom, kitchen, toilets, detergents, fabric softener
	Coating (4)	Sprays, paint supplements
	Furnishing (3)	Pillows
	Furnishing/coating (3)	Showerheads, locks, water taps
Filtration, purification, neutralization, sanitization (13)	Filtration (8)	Air filters, ionic sticks
	Cleaning (6)	Disinfectant and aerosol sprays

2.2.2 Properties of AgNPs

AgNPs in the field of nanotechnology have gained considerable interest because of their unique properties such as good conductivity, catalytic, antifungal, anti-viral, anti-inflammatory and antimicrobial activity (Panyala *et al.,* 2008). They are effective in preventing bacterial infection and retarding infection in medical based products ranging from topical ointments and bandages for wound healing, to coated stents (Chen, 2007). Additional, AgNPs have biological properties, which are important for consumer products, textiles/fabrics, food technology and medical applications. Moreover, they have unique optical and physical properties, which are claimed to have great potential for medical applications such as drug delivery, diagnostic and imaging (Wijnhoven *et al.,*

2009).However, the improvements of novel AgNPs containing products is unceasingly required.

2.2.2.1 Antimicrobial and anti-inflammatory properties

AgNPs are effective killing agents for a wide spectrum of gram-negative and gram-positive bacteria (Burrell *et al.,* 1999), including antibiotic-resistant strains (Percival *et al*., 2007). The gram-negative bacteria include genera such as *Escherichia, Acinetobacter, Salmonella, Pseudomonas* and *Vibrio*. Gram-positive bacteria include genera such as *Listeria, Bacillus*, *Staphylococcus, Enterococcus* and *Streptococcus*. The antibiotic resistant bacteria strains include vancomycin-resistant and methicillin-resistant *Enterococcus faecium* and *Staphylococcus aureus*.

Recently, it has been shown that AgNPs with diameter ranging between 5-32 nm increase the antimicrobial activity of different antibiotics (Shahverdi *et al.,* 2007). Small nanoparticles with large surface area to volume ratio simply provide a more efficient means for antimicrobial activity even at a lower concentration. Triangularly shaped AgNPs display the strongest antimicrobial activity (Wijnhoven *et al.,* 2009). AgNPs are more effective and fast acting fungicides against a wide spectrum of common fungi including *Aspergillus, Candida,* and *Saccharomyces*. In addition, these nanoparticles are effective against yeast isolated from bovine mastitis (Wijnhoven *et al.,* 2009). AgNPs with diameters between 5-20 nm exhibit inhibition of HIV-1 virus replication (Sun *et al.,* 2005) whereas, gold nanoparticles with average diameter 1-10 nm show a relatively low anti-HIV-1 activity (Elechiguerra *et al.,* 2005).

In animal models, AgNPs have the ability to alter the expression of matrix metallo-proteinases (proteolytic enzymes that play crucial roles in different inflammatory and repair processes), suppress the expression of tumour nicrosis factor (TNF)-α, interleukin (IL)-12, and IL-1b, and induce apoptosis of inflammatory cells (Bhol and Schechter, 2005). In addition, these nanoparticles modulate cytokines that are involved in wound healing (Wijnhoven *et al.,* 2009).

2.2.3 Synthesis of metallic nanoparticles

Two methods or approaches have been widely applied to synthesized metallic nanoparticles namely, the top-down and the bottom-up approaches.

2.2.3.1 Top-down approach

The principle behind the top-down approach is to take a bulk piece of the material and change it into the desired nanomaterial (Figure 2). The fabrication techniques include cutting, grinding and etching, which have been developed to work on the nano-scale. Top-down techniques can produce nanomaterials with a size ranging between 10-100 nm (Kildeby *et al.,* 2005). Nonetheless, top-down often results in nanomaterials with rough surfaces. These imperfect surface structures affect the physical properties and surface chemistry of the nanomaterials negatively because of high surface to volume ratio. This approach is however, important when highly complex structures are desired (Kildeby *et al*., 2005).

2.2.3.2 Bottom–up approach

The bottom-up or self-assembly approach refers to the construction of a structure atom-by-atom, molecule-by-molecule or cluster-by cluster (Figure 2). A good example of the bottom-up approach is colloidal dispersions, which are used to synthesize the nanoparticles. The sizes

of the nanomaterials, which can be obtained through this approach, span the full nano-scale. The bottom-up approach is advantageous because of its better possibilities to obtain nanomaterials with less defects and more homogeneous chemical compositions. This is due to the mechanisms utilized in the synthesis of nanostructures that reduce the Gibbs free energy, so that the resulting nanomaterials are in a state closer to thermodynamic equilibrium (Kildeby *et al.*, 2005).

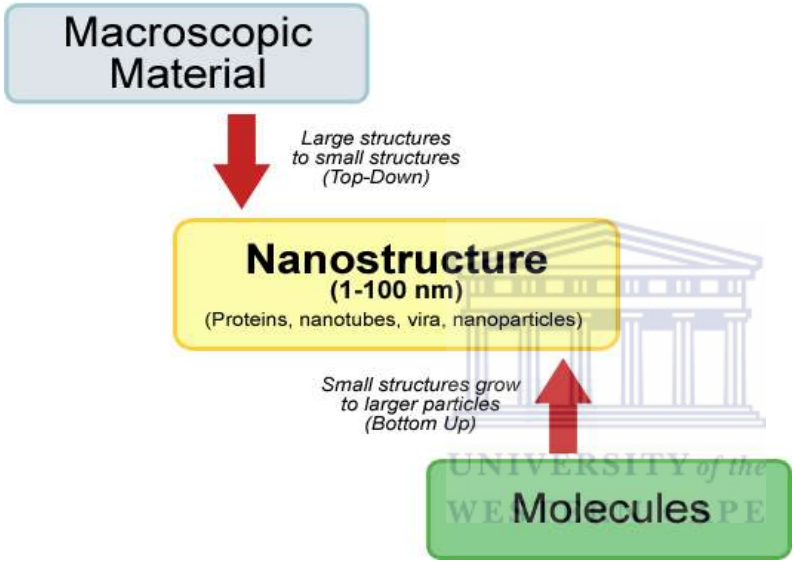

Figure 2: The top-down approach vs. the bottom-up approach for synthesis of nanoparticles (Kildeby *et al.*, 2005)

2.2.3.3 Synthesis of AgNPs

The synthesis of AgNPs can be done using a bottom-up approach. This approach provides an opportunity to produce AgNPs in the range of 1-100 nm (Daniel and Astruc, 2004). It also gives an advantage of producing stable AgNPs compared to AgNPs produced by the top-down approach, because the nanoparticles are formed as defined crystalline structures (Balzani, *et al.,* 2002). The stability of nanoparticles is of significance when examining and exploiting their properties. AgNPs can be synthesized by chemical reduction, photochemical reduction, metallic wire explosion, sonochemical method and polyol method (Jones *et al.,*

2011). The simplest and the most commonly used method for preparing metal nanoparticles is the chemical reduction of metal salts. In the following section, various synthesis methods from the literature will be reviewed.

2.2.4 Chemical reduction

2.2.4.1 Metal salts: Hydrazine and formaldehyde

The chemical reduction method involves the reduction of the metal salts in the presence of an appropriate capping agent, which is essential for controlling the growth of metal colloids and preventing them from agglomerating. Synthetic polymers such as polyvinylpirrolidone (PVP), polyvinylalcohol (PVA) and gelatin are often used as protecting agents. The reduction of silver nitrate with alkyl acid phosphate in the presence of gelatin can produce particle sizes of 0.1-1.0 nm. It has been shown that vinyl polymers possess better protecting characteristics over substances such as gelatin (Nersisyan *et al.,* 2003). The reduction of pre-heated silver nitrate solution in the presence of PVP results in silver powder with a particle size of ~300 nm. The size of these particles can be reduced to 100 nm, if the reduction of silver nitrate is done by hydrazine in the presence of PVP. An aqueous solution of 0.01 M silver nitrate in the presence of PVP and PVA reduced with formaldehyde permitted the formation of colloidal dispersion of silver with the particle size ranging between 7-20 nm (Kan-Sen and Chiang-Yuh, 2000). It was noted that a low concentration of initial solutions of silver with a large quantity of PVP, negativity influenced the quality of the product and efficiency of the process (Nersisyan *et al.,* 2003).

2.2.4.2 Citrate, ascorbic acid or borohydride

Reducing agents such as citrate (Pillai and Kamat, 2004), ascorbic acid (Sondi *et al.,* 2003) and borohydride (Ahmadi *et al*., 1996) are among the most widely used reductants for the

reduction of silver nitrate in aqueous solutions. AgNPs prepared with citrate produced spherical and rod-like particles. This is because of competition of nucleation in the growth processes (Dong *et al.,* 2009). Conversely, AgNPs prepared by borohydride produced small spherically shaped particles of less than 10 nm due to high reactivity of the reducing agent, which induces an explosive nucleation process. The change of reaction parameters such as molar ratio of the reductant or silver precursor, pH, or temperature of the reactions when using citrate or borohydride, affects the nucleation and growth processes and thus the sizes of the AgNPs (Qin *et al*., 2010). When synthesizing gold nanoparticles by reducing $HAuCl_4$ with citrate, variation in molar ratio of citrate/$HAuCl_4$ or pH is effective to tune the reactivity of the gold precursor (Ji *et al.,* 2007). In addition, it is easy to mediate the growth stage and nucleation and prepare gold nanoparticles with various sizes by changing the molar ratio or pH of the reactions. A reasonable way to prepare AgNPs with tunable size is to choose a reductant with suitable reactivity to control the nucleation growth processes of the particles (LaMer and Dinegar, 1950).

2.2.5 Point of zero charge

The point of zero charge (PZC) is the most imperative surface parameter used to characterize the acid-base behaviour of solids, mainly mineral oxides in electrolytic suspensions (Vakros *et al.,* 2002). It can be described as the pH value at which the metal surface charge is zero, meaning that at this pH the charge of the positive surface sites are equal to the charge of the negative ones (Fernández-Nieve *et al.,* 1998). However, since this parameter has many applications, for instance in case where oxides are used as supports for preparing supported catalyst, few techniques have been established so far for its experimental determination. The widely used techniques are potentiometric titrations (PT), mass titration (MT) and the immersion techniques (IT). Potentiometric titrations measure the dependency of the

equilibrium while mass titration determines the point of zero charge of mineral hydroxides immersed in electrolyte. The use of the immersion technique results in low accuracy (±1 pH unit), while the mass titration technique demands quite a large amount of the solid, which may not be available. The new technique for the determination of PZC is potentiometric mass titrations technique (PMT). This technique is quite similar to the PT technique; the main difference is that in the PMT technique, the potentiometric curves are determined for three different values of the mass of the oxide immersed in the electrolyte solution, keeping constant the ionic strength of the solution (Vakros *et al.,* 2002).

2.2.6 Stabilizing agents

2.2.6.1 Polyvinylpyrrolidone

Polyvinylpyrrolidone (PVP) is a linear polymer and stabilizes the nanoparticles surface via bonding with the pyrrolidone ring. In addition, PVP is water soluble, un-charged, non-toxic, and, has often been used in different medical applications (Lee Ha-Young *et al*., 2008). However, the PVP backbone has important hydrophobic moieties (i.e. 6 carbons per monomer unit) that are also hydrophobic, resulting in precipitation due to increase of salt concentration (Song *et al.,* 2011). Infrared (IR) and X-ray photoelectron spectroscopic (XPS) studies have shown that oxygen and nitrogen atoms of the pyrrolidone ring can result in the PVP chain being absorbed into the surface of silver. A study by Wu *et al.,* (2010) uncovered the existence of Ag^{+}-O interaction, and demonstrated that the Ag^{+} -PVP is formed through the coordination between Ag^{+} and oxygen in the carbonyl group. This facilitates the exchange of electrons between Ag^{+} and the adjacent N atom found on the pyrrolidone ring. Moreover, N atoms with lone pair electrons serve as an electron donor, eventually leading to the reduction of Ag^{-} to form PVP-capped Ag nanoparticles (Wu *et al.,* 2010).

2.2.6.2 Citric acid

Citric acid is a small molecular weight carboxylic acid that is very hydrophilic and miscible in water. Additionally, citric acid is the most common organic substance in the natural environment and our daily lives (e.g., fruit juice). Citric acid keeps nanoparticles well separated with a nominal size of 10~20 nm. Therefore, developing an understanding of the mechanism as well as the effects of AgNPs capped with citrate would contribute towards evaluating the fate and impact of AgNPs in the environment matrixes (Lee *et al*., 2012).

2.2.7 Photochemistry

Photochemistry involves the use of a chemical reaction that utilizes light to initiate transformation (Hoffmann, 2008). Energy is absorbed or emitted by matter in discrete quanta called photons. The absorption of light leads to an electronic excitation from ground state to excited state. A variety of photoreactions with high selectivity, chemical yields and photon efficiencies have been developed. Due to its easy generation, control and handling, light is also considered a clean and traceless reagent. However, photochemical reactions for chemical production processes are quite rare, and most technical processes are limited to commodity chemicals (Oelgemöller and Shvydkiv, 2011).

2.2.8 Techniques to characterize AgNPs

Techniques such as UV-vis and TEM can be used to characterise AgNPs.

2.2.8.1 Ultra-Violet-Visible spectroscopy (UV-vis)

UV-vis is a valuable tool for characterizing the structure of AgNPs (Guzman *et al.,* 2012). It is widely known that Surface Plasmon Resonance (SPR), which causes shifts to longer wavelengths with increasing particle size, relate to the optical absorption spectra of metal

nanoparticles. However, the absorbance of AgNPs depends mainly on their sizes and shapes. Generally, when the symmetry of the nanoparticles increases it leads to the decrease in the number of SPR (Guzman *et al.,* 2012). Correlation studies of the absorption spectra of individual AgNPs with their sizes (between 40-120 nm) and shapes (triangular truncated pyramids, spheres, decahedrons and platelets) showed that spherical and roughly spherical nanoparticles, decahedral or pentagonal nanoparticles, and triangular truncated pyramids and platelets absorbed in both the blue-green and red part of the UV-Vis spectrum respectively (Mock *et al.,* 2002).

2.2.8.2 Transmission Electron Microscopy

Transmission Electron Microscope (TEM) is a technique that enables the imaging of the crystallographic structure of a sample at an atomic scale. This technique allows the determination of nanoparticle geometry and gap size with less than 0.2 nm resolution. Because of its high resolution, it is a valuable tool for studying nanoscale properties of crystalline material such as semiconductors and metals. At this nanoscale, crystalline defects and individual atoms can be imaged. Since crystal structures have 3-dimensions, it is necessary to combine various views of the crystal, taken from different angles into a 3D map. TEM shows AgNPs that are spherical in shape with smooth surface morphology and it shows that the produced AgNPs are uniform in size and shape (Das *et al.,* 2009).

2.3 *Saccharomyces cerevisiae*

S. cerevisiae is amongst the most studied species of unicellular fungi. *S. cerevisiae* is an excellent model organism for assessing gene regulation of more complex eukaryotic organisms (Henry and Patton, 1998). It is used to ferment sugars of rice, wheat, barley and corn to produce alcoholic beverages in the baking industry. It is also been utilized to expand

or raise dough. *S. cerevisiae* is easy to cultivate, and can be genetically manipulated. It is readily available in grocery stores and inexpensive. *S. cerevisiae* was the first eukaryotic organism whose genome was completely sequenced, annotated and made publicly available. The availability of the complete genome sequence of this yeast made it possible to develop many novel tools for evaluating all molecular components of the cell and their interactions. Although mammalian cells share similar homologies with the yeast, some compounds assayed to be non-toxic for *S. cerevisiae* may be toxic to human cells and tissues. An example of homologous proteins in yeast and humans is the inducible multidrug resistance ABC transporter pdr5p (Tutulan-Cunita *et al.,* 2005). This transporter protein is able to export a broad range of chemically distinct compounds (Välimaa *et al.,* 2008).

2.3.1 The growth curve of *S. cerevisiae*

Yeast cell division occurs by budding in which a daughter cell is initiated as an out-growth from the mother cell, followed by nuclear division, formation of cell wall and cell separation (Werner-Washburne *et al.,* 1993). Yeast cells grow in three main phases namely; the lag phase, the exponential and the stationary phases. In the lag phase, there is no apparent growth but the cells are adapting to their new environment and synthesizing chemicals and enzymes necessary for growth (Longo *et al.,* 1996). The exponential phase, occurs where the growth rate is at a maximum, but is kept under control by environmental factors (Werner-Washburne *et al.,* 1993). In the stationary phase, one or more components of nutrients gets depleted, metabolism slows down and cells stop rapid division(Werner-Washburne *et al.,* 1996; Longo *et al.,* 1996).

Since there is an increased amount of toxic chemicals present in our daily lives, a sensitive, robust, rapid and cheap toxicity assay is needed for assessing acute toxicity in eukaryotic cells. This topic has been studied extensively and many biological toxicity tests developed. In

addition, Bitton, (1983) has reviewed the microbial and biochemical tests for evaluating chemical toxicity especially in the aquatic environment. Since then, several models such as insect (Nascarella *et al.,* 2003), fish (Pichardo *et al.,* 2007), *Daphnia magna* (Zurita *et al.,* 2007) and tumor cell lines (Cheung *et al*., 2006) have been used to evaluate the toxicity of molecules in eukaryotic cells and tissues. However, none of the above models can answer the demands for a general model, which is more accurate in predicting the effects of toxic chemicals against humans. Model organisms from various species have different sensitivities, which implies biological tests will differ more or less from one species to other and may not give general results when assessing toxicity (Codina *et al.,* 1993). Moreover, using such biological systems to evaluate the toxicity of silver in fat-soluble (highly hydrophobic) compounds is difficult, since the presence of this compound may be underestimated (Välimaa *et al.,* 2008).

2.3.2 Tetrazolium salts

The use of tetrazolium salts like WST-1, XTT and MTT, have gained grounds in cell biology for measuring the metabolic activity of various cells from mammalian to microbial origin. These salts are used as indicators of cellular proliferation and biomass for both eukaryotic and prokaryotic cells (Johnsen *et al*., 2002; McCluskey *et al.,* 2005). XTT is a colourless tetrazolium salt, converted into a coloured, water soluble formazan which is derived from dehydrogenase, with succinate dehydrogenase being particularly important (Kuhn *et al*., 2003). Succinate dehydrogenase plays a crucial role in the supply of energy to cells. Unlike other tetrazolium salts (such as CTC and TTC), XTT forms a soluble formazan and does not need extraction.

Colorimetric methods are attractive because they possess the potential to generate clear cut end-points based on the visible colour change. Additionally, they allow for the rapid

assessment of samples by a large number of tests for toxicity very quickly (Koban *et al.,* 2012). The living cells reduce the tetrazole ring, which results in a coloured formazan product and can be easily assessed visually and quantified with a spectrophotometer. These assays were used to test the efficiency of antifungal drugs in killing or inhibiting the growth of *Candida albicans* as well as other fungi (Kuhn *et al*., 2003). The tetrazolium salts used in biology are aromatic derivatives of 1,2,3-tetrazole and include monotetrazoliums like 2,3-bis(2-methoxy-4-nitro-5-sulfophenyl)-2H-tetrazolium-5-carboxanilide inner salt (XTT), 2-(4,5-dimethyl-2-thiazolyl)- 3,5-diphenyl-2H-tetrazolium bromide (MTT) and 2-(4-iodophenyl)-3-(4-nitrophenyl)-5-(2,4-disulfophenyl)-2H-tetrazolium monosodium salt (WST-1) (Knight*, et al*., 2006). WST-1 and XTT are reduced to form a soluble coloured formazan product, capable of crossing cellular membranes.

2.3.3 Toxic effects of AgNPs on environment

AgNPs are generally disposed in aquatic environments during manufacturing, use or waste recycling. These disposed particles easily get absorbed by algae, which form the basis of most aquatic food. The absorbed particles can thus be easily transferred up the food chain through herbivorous crustacean, grazing fish and humans. Studies have revealed that AgNPs accumulate in the microalga *Chlamydonas* and transfer to the zooplanktonic crustacean, *daphnia*, which feed on the algae (Dash *et al*., 2012).

2.3.4 Effect of silver nanoparticles on the aquatic food-chain.

2.3.4.1 Microalga (chlamydonas)

Algae are one of the most important component of the environment and ecosystem which serve as primary producer, contributing 40% of the global productivity of biomass (Ji *et al*.,

2011). This component has been used as bio-fertilizer, biofuel, pollution control agent (e.g algae bioreactors), casein stabilizer as well as source of nutrition (B complex, vitamins and minerals). Only a few studies evaluated the effect of AgNPs on unicellular micro-algal growth, such as *Chlamydomonas* and marine diatom *Thalassiosira*. The reactivity of AgNPs against algal components can have an impact on algal photosynthetic enzymes. In addition, these nanoparticles have been shown to have an effect on chlorophyll content, and nuclear division leading to chromosomal aberrations and cell wall damage (Dash *et al.,* 2012).

2.3.4.2 Zooplanktonic crustacean Daphnia magna

Daphnia magna (D. Magna), which is a freshwater filter-feeding crustacean, is considered as the most sensitive organisms used to study ecotoxicity. Since *D. magna* is found at the bottom of the food-chain in aquatic ecosystems, any change that can take place in its population quality or quantity can result in changes in the population of other organisms feeding on it. Although various studies have evaluated the toxicity of AgNPs in aquatic animals such as Daphnia, the distinct characteristics of nanoparticles (e.g. capping agent, preparation method, size and shape) may change their effect on living organisms (Asghari *et al.,* 2012).

2.3.4.3 Cyprinus Carpio

The common carp *Cyprinus carpio* is one of the more abundant species found in the freshwater environment. Due to its large size, carp have a better capacity for resistance to pollutants compared to other laboratory fish including zebrafish and Japanese medaka. Carp species are not used to examine the effects of exposure to low-dose of pollutants. However, they are being considered as one of the most suitable models for assessing the non-fatal effects of pollutants by evaluating changes in fish physiology and histology or fluctuations in

anti-oxidant enzyme systems (which are responsible for eliminating the oxidation stress during the early stage of the body's defensive mechanism). One impact possessed by AgNPs is the inhibition of the oxygen/carbon dioxide exchange process due to the injury of the respiration organs (gills). The study by Lee *et al*., (2012), has shown that the exposure of fish to AgNPs initially cause the bifurcation of the filament, and increase in mucous cells number and size, and hyperplasia of the lamella epithelium (Lee *et al.,* 2012).

2.3.5 Toxic effects of silver and AgNPs on health

Silver has potential toxic effects on human health and it enters the body through several portals. Previous studies have indicated that silver ions (Ag^+) cause early changes on the cell membrane permeability to potassium ion (K^+) and sodium ion (Na^+)at concentrations that do not limit Na^+, K^+, -ATP activity (Kone *et al,* 1988). Forits part, AgNPs have intensive effect on the expression and proliferation of cytokine by peripheral blood mononuclear cells (PBMCs) (Seung-hoen *et al.,* 2006). At concentrations above 15 mg/L, AgNPs have a significant cytotoxic effect on PBMCs and phyto-haemaglutinin-induced cytokine production is inhibited (Shin *et al*., 2007).

2.3.5.1 Effects on tissues and organs

Over-exposure to silver can cause accumulation in the liver, skin, kidney, corneas, gingival, mucous membranes, nails and the spleen (Sue *et al*., 2001). Silver ions have a high affinity for thiol in the liver. The accumulation of silver can have toxic effects on organs and tissues. AgNPs can bind to different organs or tissues and cause potential toxic effects like production of reactive oxygen species (ROS) and cell activation, leading to inflammation and apoptosis (Xia *et al.,* 2006). Gopinath *et al.,* (2008) showed that nanoparticles could easily pass through cell membranes and cause severe effects on human health. High concentrations (>44.0 µg/ml)

of AgNPs are necrotic to cells, leading to fast cell membrane rupture. Furthermore, nano sized particles can easily pass through the blood-brain and blood-testes barriers due to their small size (Gopinath *et al.,* 2008). Elemental AgNPs have been found to enter the body and be distributed throughout the body via the cardiovascular system. Further, systematic and pulmonary distribution of inhaled ultra-fine elemental AgNPs in rats were found in the lungs immediately after the end of the exposure and a significant amount in the blood system, liver, kidney, spleen, heart and brain.

2.3.5.2 Effects on central nervous system

Silver is spread heterogeneously in the central nervous system (CNS). It can enter the system through the blood-brain barrier and accumulate in the large motoneurones of the brainstem and spinal cord, and in neurons found in the cerebellar nuclei and glia. The biological half-life of silver in the central nervous system is longer than in other body organs and can ultimately cause toxic outcomes on the CNS (Panyala *et al.,* 2008).

2.3.5.3 Respiratory effects

The respiratory system is a major organ that allows the entry of nanoparticles. Particles larger than nanoparticles are generally trapped by a microcilliary system in the respiratory tract. Ultra-fine particles like nanoparticles unfortunately, simply bypass the microcillary system and are deposited directly in the alveolar space (Chen, 2007). At the alveolar region these nanoparticles can be submersed into the surfactant lining of alveoli producing surface radicals and reactive oxygen species (ROS) which are harmful to the surfaces of alveoli. Some studies indicated that exposure of nanoparticles in lung epithelial cells and also in alveolar microphage cells induces oxidative stress. The toxic effects of nanoparticles are due to their intensive catalytic activity. Due to large surface area and oxidative properties, AgNPs can

produce highly reactive species like ROS in the intra-alveolar spaces. Through the interactions with the surfaces of alveoli, silver can cause irritation in the respiratory tract (Panyala *et al.,* 2008).

2.3.5.4 Argyria and argyrosis

Argyria occurs when metallic silver is deposited under skin and abdominal viscera causing it to turn ashen-grey (irreversible pigmentation) while argyrosis is the pigmentation of the eyes (Brandt and Park, 2005). These two cases are caused by placing silver-containing materials into the body or skin or by use of medicines containing silver. Argyria and argyrosis maybe localized or generalized. The localized argyria is commonly caused by the direct contact of silver and substances containing silver. Small particles can enter though sweat glands or needle punctures. However, the most affected areas are mucous membranes, eyes and hands. The symptoms of generalized argyria include pigmentation on the skin, eyes, face, V of the neck, bald scalp, waist, hands, nails and forearms (Brandt and Park, 2005). Light microscopy has revealed fine granules clustered together in the periadnexal basement membrane and dermal elastic fibres. Additionally in generalized argyria, the degree of slate-grey cutaneous discolouration differs from barely perceptible to pronounced silver that contains granules deposit in and around cutaneous adnexal structures. These granules were shown to consist of silver sulphide (Panyala *et al.,* 2008).

2.3.6 Silver nanoparticles, the disruptor of basal cell functions.

In vitro studies have revealed that AgNPs are able to enter cells through phagocytosis or passive diffusion through cell membrane. Once the AgNPs are in the cell cytoplasm, they appear in intracellular vesicles and are able to enter organelles such as mitochondria and nuclei. The entrance of AgNPs and their toxic potential in a cell depends on their sizes. A

study by Wei *et al*., (2010) showed that silver micro-particles (2-20 μm) did not gain entry in mouse fibroblast cells, whereas AgNPs with the diameter of 50-100 nm were found inside the same cell. On the other hand, studies comparing different sizes of AgNPs have shown smaller particle to be more cytotoxic (Whitacre, 2013).

The treatment of rat alveolar microphages with hydrocarbon coated spherical AgNPs with the primary size of 15 nm increased ROS and depleted glutathione S-transferase (GST) level. However, this could result from AgNPs reacting with GST-maintenance enzyme leading to an increase in ROS levels and the accompanied depletion of GST levels producing oxidative stress.ROS are responsible for activating the cascade leading to programmed cell death (apoptosis). Apoptosis result from moderate oxidative stress while severe stress results in necrosis. Necrosis is associated with inflammation and can be characterized by swelling and lysing of cells, whereas apoptosis is an active cellular process that leads to morphological cell changes (e.g. cell shrinkage, membrane blebbing, nuclear condensation, DNA fragmentation) and to the formation of apoptotic bodies that are engulfed by phagocytic cells (Whitacre, 2013).

References 1

1. Ahmadi, T.S., Wang, Z.L., Green, T.C., Henglein, A. and El-Sayed, M.A. Shape-controlled synthesis of colloidal platinum nanoparticles. *Science*. (1996); **272**: 1924–1925.
2. Asghari, S., Johari, S.A., Lee, J.H., Kim, Y.S., J, Y., Choi, H.J., Moon, M. and Yu, I.J. Toxicity of various silver nanoparticles compared to silver ions in *Daphnia magna*. *Journal of Nanobiotechnology*. (2012); **10**:1-14.
3. Balzani, V., Credi, A and Venturi, M. The Bottom-Up approach to molecular-level devices and machines. *Chemistry European Journal*. (2002); **8**: 5525-5532.
4. Bhol, K.C and Schechter P.J. Topical nanocrystalline silver cream suppresses inflammatory cytokines and induces apoptosis of inflammatory cells in a murine model of allergic contact dermatitis. *Br Journal of Dermatology*. (2005); **152**:1235-1242.
5. Bitton, G. Bacterial and biochemical tests for assessing chemical toxicity in the aquatic environment: A review. *CRC Critical Review and Environmental Control*. (1983); **13:** 51-67.
6. Brandt, D., Park, B., Hoang, M. and Jacobe, H.T. Argyria: secondary to ingestion of home made silver solution. *Journal of American Academy Dermatology*. (2005); **53**: 105-107.
7. Braydich-Stolle, L., Hussain, S., Schlager, J.J. and Hofmann, M.C. *In vitro* cytotoxicity of nanoparticles in mammalian germ-line stem cells. *Toxicological Science.* (2005); **88**: 412–419.
8. Burrell, R.E., Heggers, J.P., Davis, G.J. and Wright, J.B. Efficacy of silver-coated dressings as bacterial barriers in a rodent burn sepsis model. *Wounds*. (1999); **11**:64-71.

9. Chen, X and Schluessener H.J. Nanosilver: A nanoproduct in medical application. *Toxicology Letter*. (2007); **176**: 1-12.

10. Cheung, R.Y., Rauth, A.M., Ronaldson, P.T., Bendayan, R. and Wu, X.Y. *In vitro* toxicity to breast cancer cells of microsphere-delivered mitomycin C and its combination with doxorubicin. *Journal of Biopharmaceutical*. (2006); **62**: 321-331.

11. Codina, J.C., Perez-Garcia, A., Romero, P. and de Vicente, A. A. Comparison of microbial bioassays for the detection of metal toxicity. *Architecturer Environmental Contamination Toxicology*. (1993); **25**: 250-254.

12. Cui, Y., Wei, Q., Park, H. and Lieber, C. Nanowire nanosensors for highly sensitive and selective detection of biological and chemical species. *Science*. (2001); **293**: 1289–1292.

13. Daniel, M.C and Astruc, D. Gold nanoparticles: assembly, supramolecular chemistry, quantum-size-related properties, and applications toward biology, catalysis, and nanotechnology. *Chemical Revolution.* (2004); **104**: 293–346.

14. Dankovich, T.A. and Gray, D.G. Bacterial paper impregnated with silver nanoparticles for point-of-use water treatment. *Environmental Science and Technology.* (2011); **45**:1992-8.

15. Das, R., Nath, S. S., Chakdar, D., Gope, G. and Bhattacharjee R. Preparation of silver nanoparticles and their characterization. *Journal of Nanotechnology*. (2009); **49:** 1-5.

16. Dash, A., Singh, A.P., Chaudhary, B. R. Singh, S. K and Dash, D. Effect of Silver Nanoparticles on Growth of Eukaryotic Green Algae. *Nano-Microbiology Letter.* (2012); **4**: 158-165.

17. Dong, X., Ji, X., Wu, H., Zhao, L., Li, J. and Yang, W. Shape control of silver nanoparticles by stepwise citrate reduction. *Journal of Physical Chemistry.* (2009); **113**: 6573–6576.

18. Eisler, R. A review of silver hazards to plants and animals. 4th Int. Conf. transport, fate and effects of Silver in the environment, *Madison, Wisconsin*. (1996); 143–144.

19. Elechiguerra, J. L., Burt, J. L., Morones, J. R., Camacho-Bragado, A., Gao, X., Lara, H.H. and Yacaman, M. J. Interaction of silver nanoparticles with HIV-1. *Journal of Nanobiotechnology*. (2005); **3**: 1-8

20. Fernández-Nieves, A., de las Nieves, F. J. and Richter, C. Point of zero charge for a TiO2/water interface. *Progress in colloid and polymer science*. (1998); **110:** 21-24.

21. Gopinath, P., Gogoi, S.K., Chattopadhyay, A. and Gosh, S.S. Implications of silver nanoparticles induced cell apoptosis for *in vitro* gene therapy. *Journal of Nanobiotechnology*. (2008); **19:** 1-13.

22. Gulbranson, S. H., Hud, J. A. and Hansen, R. C. Argyria following the use of dietary supplements containing colloidal silver protein. *Cutis*. (2000); **66:** 373–376.

23. Guzman, M., Dille, J. and Godet, Stéphane. Synthesis and antibacterial activity of silver nanoparticles against gram-positive and gram-negative bacteria. *Nanomedicine: Nanotechnology, Biology and Medicine*. (2012); **8**:37–45.

24. Henry, S. A. and Patton-Vogt, J. L. Genetic regulation of phospholipid metabolism: yeast as a model eukaryote. *Progress of nucleic acid research molecular biology*. (1998); **61**: 133-79.

25. Hoffmann, N. Photochemical reactions as key steps in organic synthesis. *Chemistry Review*. (2008); **108**: 1052–1103.

26. Hogstrand, C. and Wood, C.M. The toxicity of silver to marine fish. *4th International conference. Transport, fate and effects of silver in the environment Madison, Wisconsin.* (1996), pp 109–112.

27. Hunter, P. R., J. M. Colford, M. W., LeChevallier, S. and Binder, P.S. Panel on waterborne diseases. *Emerging Infectious Diseases Journal*. (2000); **7**: 544-545.

28. Ji, J., Long, Z. and Lin, D. Toxicity of oxides nanoparticles to the green algae *Chlorella spieces*. *Chemical Engineering Journal*. (2011); **170**: 525-530.

29. Ji, X., Song, X., Li, J., Bai, Y., Yang, W. and Peng, X. Size control of gold nanocrystals in citrate reduction: the third role of citrate. *Journal of American Chemistry Society*. (2007); **129**: 13939–13948.

30. Johnsen, A. R., Bendixen, K. and Karlson, U. Detection of microbial growth on polycyclic aromatic hydrocarbons in microtiter plates by using the respiration indicator WST-1. *Applied Environmental Microbiology.* (2002); **68**: 2683–2689.

31. Jones, M. R., Osberg, K. D., Macfarlane, R. J., Langille, M. R and Mirkin, C. A. Templated techniques for the synthesis and assembly of plasmonic nanostructures. *Chemical Revolution.* (2011); **111**: 3736–3827.

32. Kan-Sen, C. and Chiang-Yuh, R. Synthesis of nanosized silver particles by chemical reduction method. *Materials Chemistry and Physics.* (2000); **64**: 241–246.

33. Kildeby, N. L., Andersen, O. Z., Roge, R.E., Petersen, T. L. and Riis, J. F. Silver nanoparticles. *Institute for Physics and Nanotechnology - Aalborg University.* (2005); 9-14.

34. Knight, S. A. B. and Dancis, A. Reduction of 2,3-bis(2-methoxy-4-nitro-5-sulfophenyl)-2H-tetrazolium-5-carboxanilide inner salt (XTT) is dependent on CaFRE10ferric for *Candida albicans* grown in unbuffered media. *Microbiology*. (2006); **152**:2301–2308.

35. Koban, I., Matthes, R., Hübner, N., Welk, A., Sietmann, R., Lademann, J., Kramer, A. and Kocher, T. XTT assay of *ex vivo* saliva biofilms to test antimicrobial influences. *GMS Hospital Hygiene Interdisciplinary.* (2012); **7**: 1-10.

36. Kone, B. C., Kaleta, M. and Gullans, S. R. Silver ion (Ag+)-induced increases in cell membrane K+ and Na+ permeability in the renal proximal tubule: Reversal by thiol reagents. *Journal of Member Biology*. (1988); **102**: 11-19.

37. Kuhn, D. M., Balkis, M., Chandra, J., Mukherjee, P. K. and Ghannoum M. A. Uses and Limitations of the XTT Assay in studies of *candida* growth and metabolism. *Journal of Clinical Microbiology*. (2003); **41**: 1-4.

38. LaMer, V. K. and Dinegar, R. H. Theory, production and mechanism of formation of monodispersed hydrosols. *Journal of American Chemistry Society*. (1950); **72**: 4847–4854.

39. Lee, B., Duong, C. N., Cho, J., Lee, J., Kim, K., Seo, Y., Kim, P., Choi, K. and Yoon, J. Toxicity of citrate-capped silver nanoparticles in common carp (*Cyprinus carpio*). *Journal of Biomedicine and Biotechnology*. (2012); **12**: 1-14.

40. Lee, Ha-Young., Lee, Sang-Hoon., Xu, C., Xie, J and Lee, Jin-Hyung. Synthesis and characterization of PVP-coated large core iron oxide nanoparticles as an MRI contrast agent. *Nanotechnology*. (2008); **19:** 1-6.

41. Longo, V. D., Gralla, E.B and Valentine, J. S. Superoxide Dismutase Activity Is Essential for Stationary Phase Survival in *Saccharomyces cerevisiae. The Journal of Biological Chemistry*. (1996); **271**: 12275–12280.

42. McCluskey, C., Quinn, J. P. and McGrath, J. W. An evaluation of three new-generation tetrazolium salts for the measurement of respiratory activity in activated sludge microorganisms. *Microbiology Ecology*. (2005); **49**: 379–387.

43. Mock, J. J., Barbic, M., Smith, D. R., Schultz, D. A. and Schultz, S. Shape effects in plasmon resonance of individual colloidal silver nanoparticles. *Journal of Chemical Physics*. (2002); **116**: 6755-60.

44. Nascarella, M. A., Stoffolano, J. J. G., Stanek III, E. J., Kostecki, P. T. and Calabrese, E. J. Hormesis and stage specific toxicity induced by cadmium in an insect model, the queen blowfly, Phormia *regina* Meig. *Environmental Pollution*. (2003); **124**: 257-262.

45. Nersisyan, H. H., Lee, J. H., Son, H. T., Won, C. W. and Maeng, D. Y. A new and effective chemical reduction method for preparation of nanosized silver powder and colloid dispersion. *Materials Research Bulletin.*(2003); **3:** 8949–956.

46. Nordberg, G. and Gerhardsson, L. S. (1988). Handbook on toxicity of inorganic compounds. Marcell Dekker. New York. pp 619–624.

47. Oelgemöller M. and Shvydkiv O. Recent advances in microflow photochemistry. *Molecules*. (2011); **16:**7522-7550.

48. Panyala, N. R., Pena-Mendez, E. M. and Havel, J. Silver or silver nanoparticles: a hazadours threat to the environment and human health? *Journal of Applied Biomedicine.* (2008); **6:** 117-129.

49. Percival, S. L., Bowler, P. G. and Dolman. J. Antimicrobial activity of silver-containing dressings on wound microorganisms using an *in vitro* biofilm model. *International Wound Journal*. (2007); **4:**186-191.

50. Pichardo, S., Jos, A., Zurita, J. L., Salguero, M., Cameán, A. M. and Repetto, G. Acute and sub-acute toxic effects produced by microcystin-YR on the fish cell lines RTG-2 and PLHC-1. *Toxicology In-Vitro*. (2007); **21:** 1460-1467.

51. Pillai, Z. S. and Kamat, P. V. What factors control the size and shape of silver nanoparticles in the citrate ion reduction method? *Journal of Physical Chemistry.* (2004); **108**: 945–951.

52. Qin, Y., Ji, X., Jing, J., Liu, H., Wu, H. and Yang, W. Size control over spherical silver nanoparticles by ascorbic acid reduction. *Physicochemical Engineering Aspects*. (2010); **372:**172–176.

53. Samuel, U. and Guggenbichler, J. P. Prevention of catheter-related infections: the potential of a new nano-silver impregnated catheter. *International Journal of Anti-microbiology.* (2004); **23**:75–78.

54. Savage, N and Diallo M. S. Nanomaterials and water purification: Opportunities and challenges. *Journal of Nanoparticle Research*. (2005); **7**: 331–342.

55. Seung-heon S., Mi-kyung, Y. and Jeung-kyu K. The effects of nanosilver on the proliferation and cytokine production in peripheral blood mononuclear cells. *Japanese Journal of Rhinology*. (2006); **45**:269.

56. Shahverdi, A. R., Fakhimi, A., Shahverdi, H. R. and Minaian S. Synthesis and effect of silver nanoparticles on the antibacterial activity of different antibiotics against *Staphylococcus aureus* and *Escherichia coli*. *Nanomedicine*. (2007); **3**:168-171.

57. Shin, S. H., Ye, M. K., Kim, H. S. and Kang, H. S. The effects of nano-silver on the proliferation and cytokine expression by peripheral blood mononuclear cells. *International Immunopharmacology*. (2007); **7**: 1813-1821.

58. Sondi, I., Goia, D. V. and Matijevic, E. Preparation of highly concentrated stable dispersions of monodispersed silver nanoparticles. *Journal of Colloid Interface Science*. (2003); **260**: 75–81.

59. Song, J. E., Phenrat, T., Marinakos, S., Xiao, Y., Liu, J., Wiesner, M. R., Tilton. R. D. and Lowry, G. V. Hydrophobic interactions increase attachment of gum arabic- and PVP-coated Ag nanoparticles to hydrophobic surfaces. *Environmental Science and Technology*. (2011); **45**: 5988–5995.

60. Sue, Y. M., Lee, J. Y., Wang, M. C., Lin, T. K., Sung, J. M. and Huang, J. J. Generalized argyria in two chronic hemodialysis patients. *American Journal of Kidney Dischemistry*. (2001); **37**: 1048-1051.

61. Sun, R.W., Chen, R., Chung, N. P., Ho, C. M., Lin, C. L. and Che, C. M. Silver nanoparticles fabricated in Hepes buffer exhibit cytoprotective activities toward HIV-1 infected cells. *Chemistry Communication (Camb)*. (2005); **41**: 5059-5061.

62. Teodoro, J. S., Simões, A. M., Duarte, F. V., Rolo A. P., Murdoch R. C., Hussain S.M. and Palmeira, C. M. Assessment of the toxicity of silver nanoparticles *in vitro*: A mitochondrial perspective. *Toxicology in vitro*. (2011); **25**: 664–670.

63. Tiwari, D. K., Behari, J. and Sen, P. Application of nanoparticles in waste water treatment. *World Applied Science Journal*. (2008); **3**: 417-433.

64. Tutulan-Cunita, A. C., Mikoshki, M., Mizunuma, M., Hirata, D. and Miyakawa, T. Mutational analysis of the multidrug resistance ABC transporter Pdr5p with altered drug specificity. *Genes Cells.* (2005); **10**: 409-420.

65. Vakros, J., Kordulis, C. and Lycourghiotis, A. Potentiometric mass titrations: a quick scan for determining the point of zero charge. *Chemical Communication.* (2002); **22**: 1980–1981.

66. Välimaa, A. L., Kivistö, A., Virta, M. and Karp, M. Real-time monitoring of non-specific toxicity using a *Saccharomyces cerevisiae.* Reporter System. *Sensors*. (2008); **8:** 6433-6447.

67. Werner-Washburne, M., Braun, E., Johnston, G. C. and Singer, R. A. Stationary phase in the yeast *Saccharomyces cerevisiae. Microbiology Review*. (1993); **57**:383.

68. Werner-Washburne, M., Braun, E. L., Crawford, M. E and Vickie M. Peck. Stationary phase in *Saccharomyces cerevisiae. Molecular Microbiology*. (1996); **19:** 1159-1166.

69. Whitacre, D. M. Reviews of Environmental Contamination and Toxicology. *Springer.* (2013); **223**, 84-86.

70. WHO, "Guidelines for Drinking-water quality" (2008) Available [Online]: http://www.who.in/water sanitation health/dwq/fulltext.pdf (2010, 06/08).

71. Wijnhoven, S.W.P., Peijnenburg, W.J.G.M., Herberts, C. A., Hagens, W.I., Oomen, A.G. and Heugens, E. Nano-silver-a review of available data and knowledge gaps in human and environmental risk assessment. *Nanotoxicology,* (2009); **3:** 109-138.

72. Wu, C., Mosher, B. P., Lyons, K. and Zeng T. Reducing ability and mechanism for polyvinylpyrrolidone (PVP) in silver nanoparticles synthesis. *Journal of Nanoscience Nanotechnology*. (2010); **10:** 2342-7.

73. Xia, T., Kovochich, M., Brant, J., Hotze, M. and Sempf, J. Comparison of the abilities of ambient and manufactured nanoparticles to induce cellular toxicity according to an oxidation stress paradigm. *Nano Letters*. (2006); **8**: 1794-1807.

74. Zhang, Y. and Sun, J. A Study on the bio-safety for nano-silver as anti-bacterial materials. *China Journal of Medical Instrument*. (2007); **1**: 35–38.

75. Zurita, J.L., Jos, A., del Peso, A., Salguero, M., Cameán, A.M., López-Artíguez M. and Repetto, G. Toxicological assessment of indium nitrate on aquatic organisms and investigation of the effects on the PLHC-1 fish cell line. *Scientific Total Environmental.* (2007); **387**: 155-165.

CHAPTER 3

3.1 Problem statement

AgNPs are simple and less expensive nanomaterials. They possess antimicrobial activity that could have a negative impact on the naturally occurring microbial population when released in wastewater streams. These nanoparticles are highly toxic to mammalian cells and have been shown to damage the brain, liver and stem cells. Prolonged exposure of colloidal silver or silver salts under the skin can cause diseases. AgNPs in bulk form are extremely toxic to fish, algae, some plants, crustaceans, fungi and bacteria like the nitrogen fixing heterotrophic and soil forming chemolithotrophic bacteria. In physiological media, silver is able to release ions that interact with cell components and thus induce harmful effects on the cell. The study by Benn *et al*, (2008) has shown that silver can leak easily into wastewater treatment services and kill aquatic organisms in lakes and streams. In terms of potential effects on aquatic ecosystems, effective techniques for water purifications need to be developed to minimize AgNPs leaching into the environment. To minimize leaching, the Swedish Environmental Protection Agency (SEPA) has protested against the application of nano-silver in washing machines as an antimicrobial because AgNPs contaminated wastewater from the machines may leach into the environment. Additionally, the United State Environmental Protection Agency (USEPA) has decided to regulate the application of nanotechnology. Farmers are concerned that the antimicrobial activity of AgNPs will affect the beneficial bacteria found in soils. Despite their growing shares on the market, risks associated with exposure to AgNPs have not been researched adequately (Wijnhoven *et al.,* 2009). Therefore, there is a great need to investigate the toxicity of AgNPs in details.

CHAPTER 4

Photochemical synthesis of silver nanoparticles and their characterization

Abstract

The photoreduction of silver ions by citrate or PVP was used in this study to synthesize silver nanoparticles. Silver nitrate was photoreduced with light from an OSRAM Vitalux lamp (300 W and 230 V) in the presence of a stabilizing agent (PVP or citric acid), to yield AgNPs after about 10 min. The particles displayed excellent long-term stability. The effects of varying the concentration of stabilizing agent, time of exposure to light source, and pH were investigated. Characterization of the AgNPs was taken using UV-Vis and TEM techniques. UV-Vis results showed that the AgNPs absorbed UV-radiation between 400-500 nm and TEM images revealed the particles to be spherical and needle-like in shape. The shapes depended on synthesis conditions applied. AgNPs were therefore, successfully synthesized and characterized in this work.

4.1 Introduction

The synthesis of nanoparticles is an interesting field in solid-state chemistry. Due to their small sizes, nanoparticles display novel properties, which differ from the properties of the bulk material. The chemical reactivity of small metallic particles is strongly dependent on particle size. For the preparation of metal particles, protective agents have been used during the reduction of metal ions. Water-soluble polymers such as poly (vinyl alcohol), poly (N-vinylpyrrolidone), and poly (methyl vinyl ether) have been used as protective agents (Huang *et al.,* 1996). Many methods are used to synthesize AgNPs with various morphologies including nanowires, nanoparticles, nanotubes and nanoplates. Silver ions from silver nitrate are often adopted because they show high flexibility in the formation of AgNPs. In addition,

this route is straight forward and low-cost (Chen *et al.,* 2011). Energy sources for silver ion precipitation from silver nitrate can be from light irradiation, or thermal heat. The basic mechanisms involved are photothermal, photochemical (lamp or laser) and solvo-thermal reductions. A laser light, due to its exceptional capability in local processing and patterning, has attracted growing interest in producing AgNPs lately (Chen *et al.,* 2011).In this work, AgNPs were synthesized by reducing silver ions with OSRAM Vitalux lamp (300 W and 230 V) in the presence of PVP or citric acid (figure 3). The synthesized AgNPs were characterized by TEM and UV-Vis techniques.

4.2 Materials and Methods

4.2.1 Chemicals and equipment

The list of chemicals with their suppliers and purity used in this study are presented in Table 2, and the equipment used during experiment are shown in Figure 4.

Table 2: List of chemicals used in this study

Chemicals	Suppliers	Purity
Silver nitrate	Kimix Chemicals	99.8%
Polyvinylpyrrolidone	Sigma-Aldrich	99.0%
Citric acid	Sigma-Aldrich	100%
Ammonium hydroxide	Sigma-Aldrich	25%

4.2.2 Experimental procedures

4.2.2.1 Preparation of AgNPs

For the synthesis of AgNPs, PVP or citric acid solution was prepared as shown in Table 3. The solutions were labelled A1 to A7 and B1 to B7 for PVP or citric acid reactions respectively. 10 mL of PVP or citric acid solution was poured into a 50 mL beaker and the pH parameter adjusted to 6, 9 or 10.5, using either 1 M NH_4NO_3 or 1 M citric acid (Note: pH 9 was kept constant from (A1/B1 to A5/B5). $AgNO_3$ solution (10 mL) was added to the PVP or citric acid solution. The mixture was then exposed to the light source (OSRAM Vitalux lamp at 300 W and 230 V) at a height of 25 cm for 1, 2 or 3 h with continuous stirring. Figure 4 shows the set-up of the experiment. Sample A3/ B3 (Table 3) will be used to compare the UV-Vis results of time and pH parameters.

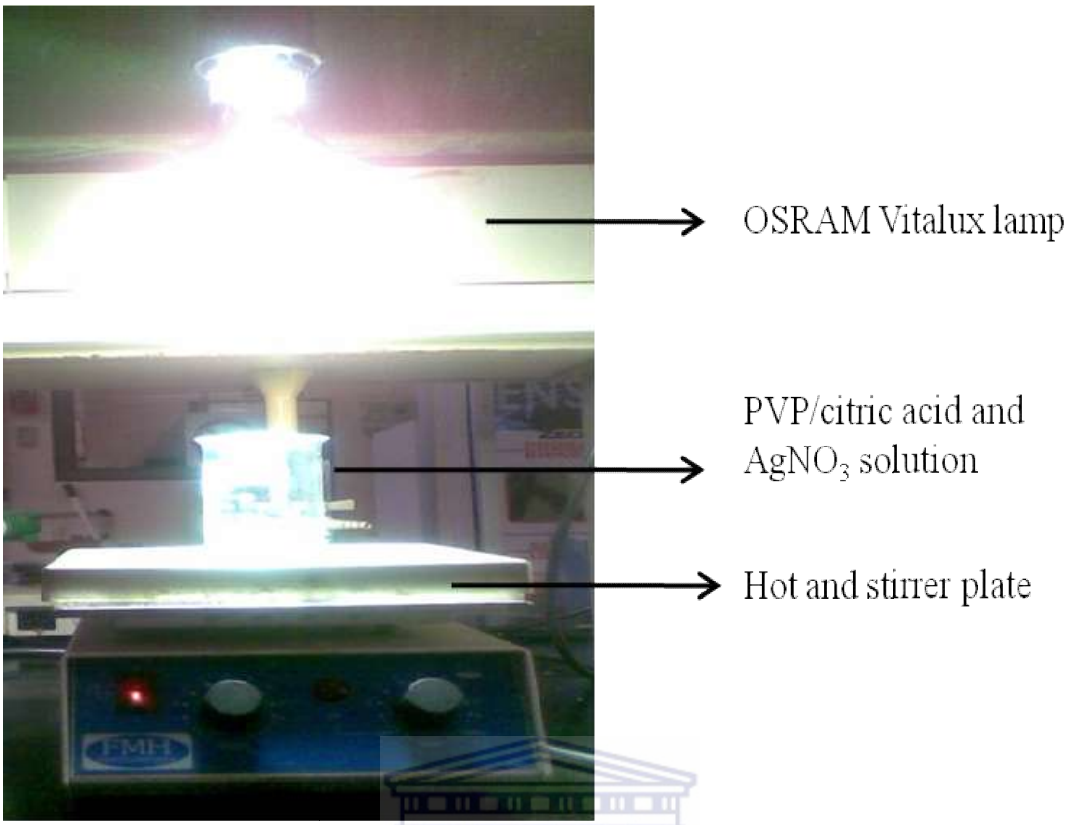

Figure 3: Experimental set-up for AgNP synthesis.

Table 3: Silver nanoparticles preparation under different conditions

Sample ID	$AgNO_3$ (mg/mL)	PVP/citric acid (mg/mL)	Time (hour)	pH
A1/B1	0.4	**0.4**	3	9
A2/B2	0.4	**2**	3	9
A3/B3	0.4	**4**	3	9
A4/B4	0.4	4	**1**	9
A5/B5	0.4	4	**2**	9
A3/B3	0.4	4	**3**	9
A6/B6	0.4	4	3	**6**
A3/B3	0.4	4	3	**9**
A7/B7	0.4	4	3	**10.5**

Table 3 presented the samples ID (A1 to A7 or B1 to B7) and applied synthesis conditions. The synthesized AgNPs were analysed by UV-Vis and TEM techniques. The red values represent the parameters that were varied to synthesize the nanoparticles.

4.2.2.2 Characterization of synthesized silver nanoparticles

AgNPs were analysed by UV-Vis, using a quartz cuvette with a 1 cm path length. A 1.5 mL of de-ionised water was transferred into the cuvette and used as blank for the spectrophotometer used. The AgNPs were analysed by transferring 1.5 mL of the sample into a cuvette and measuring its absorbance reading at OD_{600} with the spectrophotometer.

For further analysis of the AgNPs samples, TEM micrographs were obtained using TEG Technai F20 micro-analyser. A 1 μL aliquot of each AgNPs sample was placed on a carbon coated copper grid and kept under vacuum desiccation for a few minutes to dry. After drying, the copper grids were loaded onto a specimen holder. The TEM images of AgNPs samples were captured. Image J software was used to determine the particle size from which particle size distribution was plotted.

4.3 Results and Discussion

This section presents the results and discussion of the characterization of the synthesized AgNPs made with either PVP or citric acid as a dispersing agent. The effect of varying parameters such as concentration of dispersing agent, time of light exposure and pH are presented and discussed. The colour, size and shape of synthesized AgNPs are also discussed in this section.

4.3.1 Silver nanoparticles prepared in the presence of PVP

AgNPs were synthesized with PVP as dispersant according to the method described in section 4.2 Table 3. The following parameters were varied systematically: molar ratio of dispersant, time exposure to light source, and pH. All samples were exposed to the light for 1, 2 or 3 h and pH was fixed at 9 or varied between 6 to 10.5 (Table 3). UV-Vis was used to determine the size and the shape of nanoparticles and TEM images confirmed the size and their corresponding particle size distribution. Please note AgNPs colour change and UV-Vis figures are labelled (a) and (b) while TEM images and particle size distribution figures are labelled (c) and (d) respectively.

4.3.1.1 Influence of the concentration of PVP on AgNPs formation

Samples A1, A2 and A3 were obtained by respectively adding 0.4, 2 and 4 mg/mL of PVP to 0.4 mg/mL silver nitrate solution and exposing under photolight for 3 h at a pH of 9. UV-Vis and TEM were used to analyse samples A1, A2 and A3.

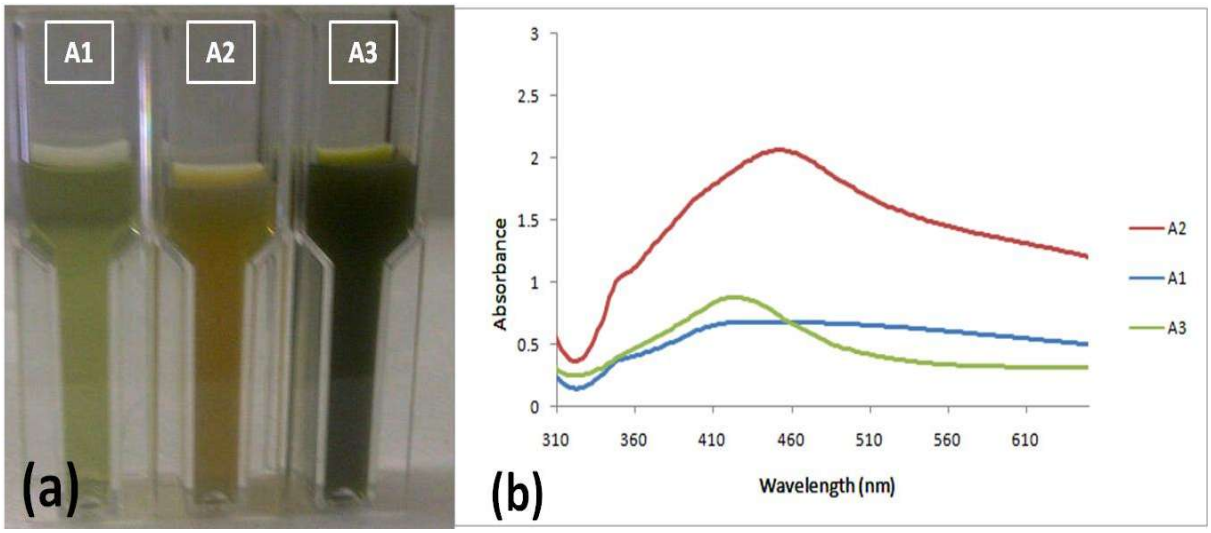

Figure 4: Synthesis of AgNPs using $AgNO_3$ with varying PVP concentrations. (a) Observable colour change at 3 different PVP concentrations. (b) UV-Vis absorbance spectra of the synthesized particles. A1, A2 and A3 represent reactions of $AgNO_3$ with 0.4, 2 and 4 mg/mL PVP respectively.

Figure 4(a) illustrates the colour change of silver nitrate and PVP solution to three shades of green (light green for A1 (0.4 mg/mL PVP), yellowish for A2 (2 mg/mL PVP) and deep green for A3 (4 mg/mL PVP) after light exposure. The change of colour indicates the synthesis of AgNPs and the different colour indicated different particle sizes and shapes.

The formation of AgNPs was further confirmed by the UV-Vis in Figure 4(b) (a valuable tool for characterizing the structures of AgNPs). Sample A1 showed a large band with low absorbance at about 430 nm and a shoulder at 380 nm, while A2 gave a band at 450 nm with highest absorbance compared to A1 and A3. The broadness of the peak in sample A1 indicates particles size distribution and the shift of absorption peak from 430 nm to 450 nm (longer wavelength) indicates bigger particle size (Brause *et al*., 2002). By increasing the concentration of the dispersing agent, the wavelength of sample A3 gave a band with high absorbance, which was blue-shifted to 420 nm indicating small particle sizes. The low absorbance observed in A1 indicated that with the molar ratio $AgNO_3$: PVP of 0.4:0.4, fewer AgNPs were formed. There were much more synthesized AgNPs with the molar ratio $AgNO_3$:

PVP of 0.4:2 (A2) and 0.4:4 (A3). These observations suggest that the dispersing agent (PVP) should be in excess to ensure the synthesis of spherically shaped AgNPs.

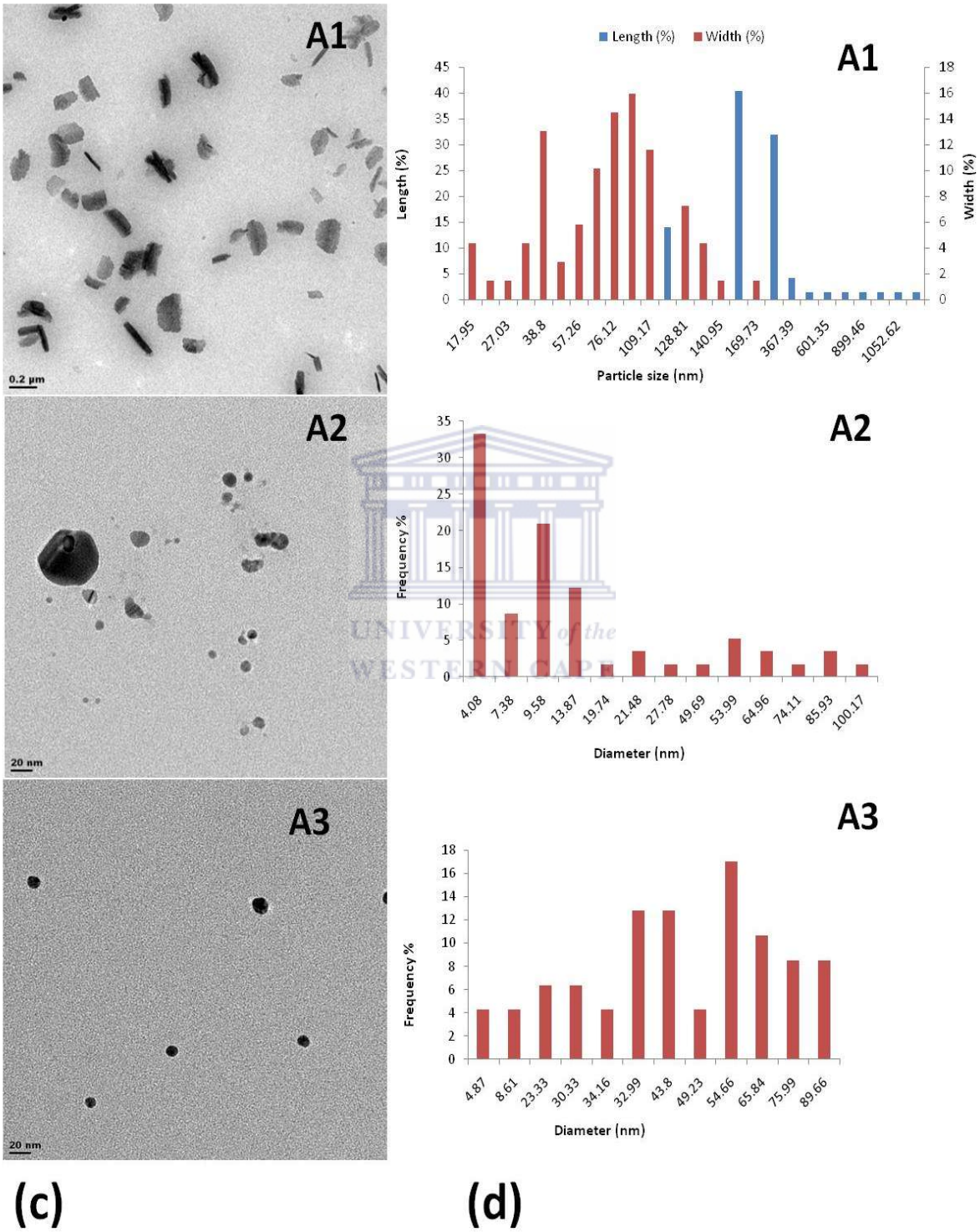

Figure 5: TEM images (c) and size distribution (d) of silver nanoparticles in A1, A2 and A3.

.

The size and morphology of AgNPs were investigated using TEM analysis. TEM images and their size distribution are shown in Figure 5 (c) and (d). The particle size distribution of sample A1 was presented (length and width) due to its needle-like shape in Figure 5 (d). Sample A1 gave an average length of about 150 nm and average width of around 90 nm. Samples A2 and A3 have an average particle size of 4.08 nm and 54.66 nm, respectively. It can be observed from TEM particle size that in sample A2 most of the nanoparticles were sized below 20 nm while A3 nanoparticles were sized between 30-60 nm. According to particle size distribution, the conditions applied to prepare A2 seemed to work the best compared to A1 and A3 because of its small particle size.

4.3.1.2 Influence of light exposure time on the formation of silver nanoparticles.

Samples A4, A5 and A3 were obtained by exposing silver ions and PVP solution to photolight for 1, 2 and 3 h, respectively. A visual colour change was observed. UV-vis and TEM were used to investigate the sizes and shapes of the synthesized AgNPs.

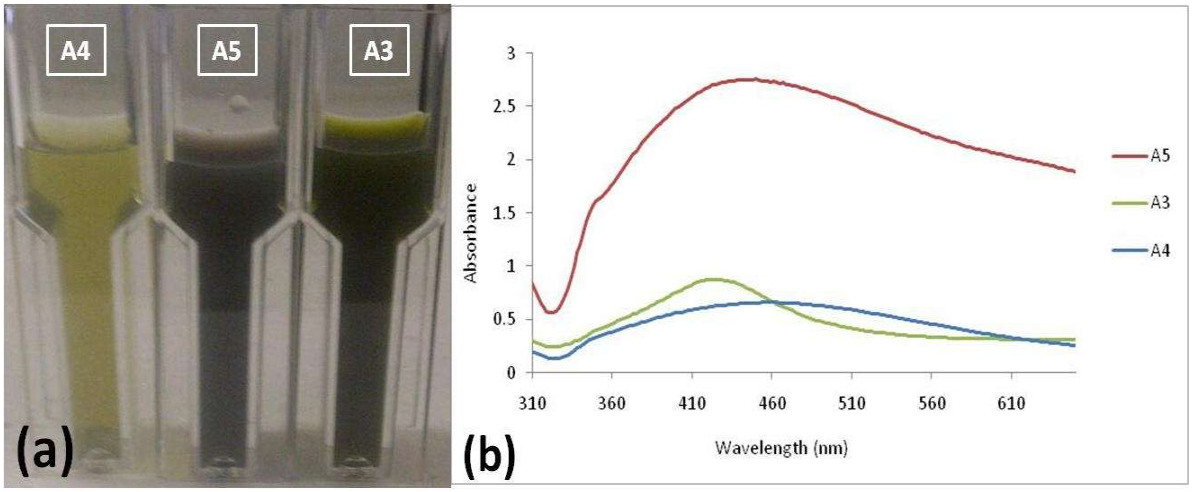

Figure 6: Colour change (a); UV-Vis absorbance (b) for AgNPs in sample A4, A5 and A3.

In figure 6 (a), an observable colour change from the colourless solution of PVP with silver nitrate to yellow, black and deep green for samples A4, A5 and A3, respectively was obtained. The change of colour indicates the potential formation of AgNPs. The colourless solution of PVP with silver nitrate, when exposed to light for 1 h resulted in a yellow colour, which indicates the initiation of AgNPs formation. As the time of reaction increases to 2 h, the colour changes from yellow to black, and from black to green with further increase in exposure time to 3 h. The results of Figure 6 (a) correlates to those obtained by Shameli *et al,* (2012) using phytosynthesis method.

The UV-vis spectrum obtained in Figure 6 (b) showed that with 1 h (A4) of light exposure there was low absorbance at a wavelength of about 460 nm. By increasing the time of light exposure to 2 h (A5), the absorbance band shifted to the shorter wavelength (blue shift) of 430 nm indicating small particles size. After increasing the time of light exposure to 3 h, A3 showed a well-defined surface plasmon band centered at a wavelength of about 420 nm. Previous studies by Huang *et al.,* (1999) using a photochemical reduction method showed that the increase of time exposure caused the absorbance peak to gradually shift towards shorter wavelengths. There is a similar trend observed with the results presented in Figure 6 (b) as it could be seen that by increasing the time of light exposure, the absorbance band blue-shifted from 460 (A4) to 430 (A5) nm and A3 has also blue-shifted from 430 (A5) to 420 (A3) nm.

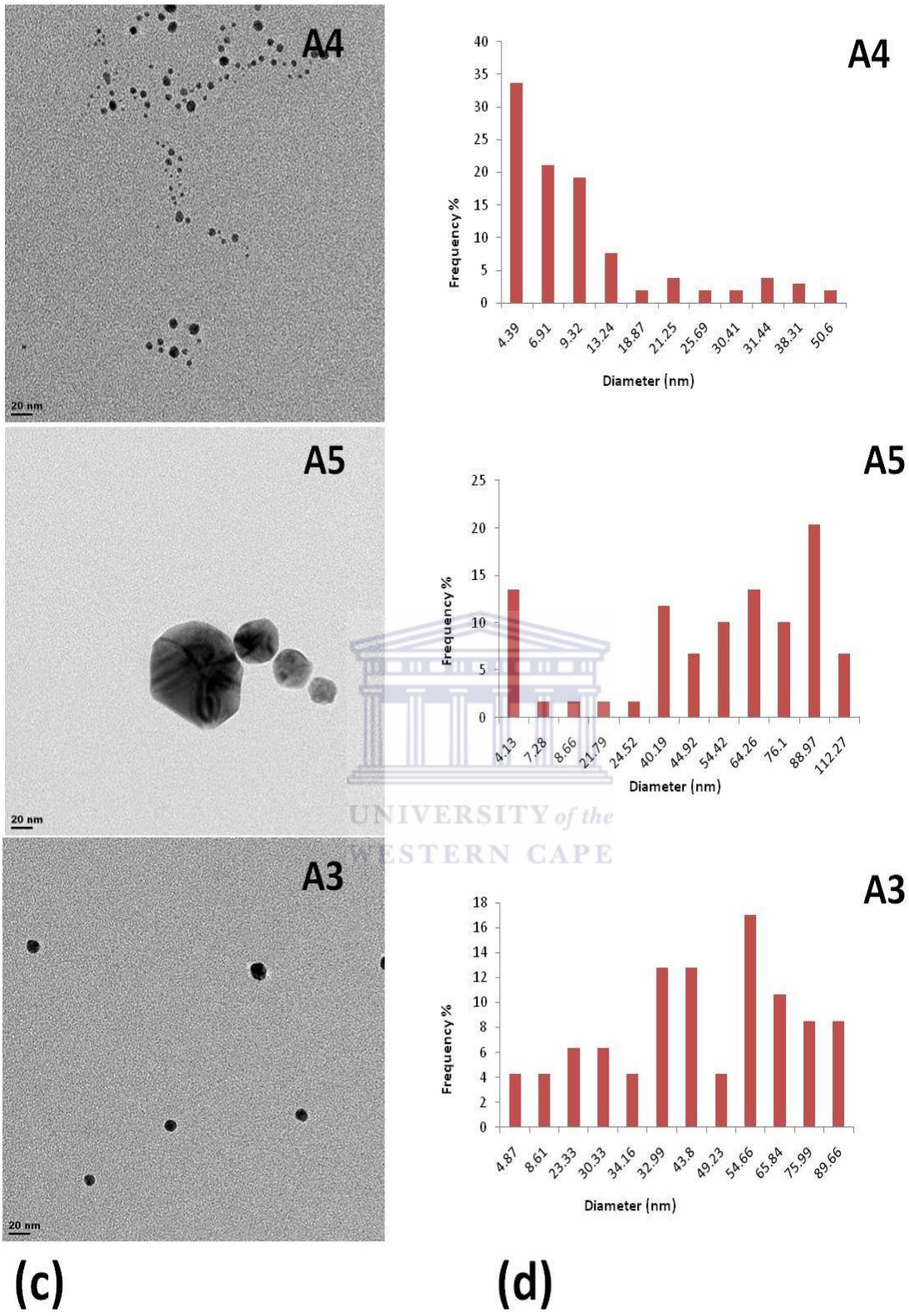

Figure 7: TEM analysis of AgNPs formed at varying photolight exposure time. (c): Images and (d) size distribution of silver nanoparticles in A4, A5 and A3.

The TEM images and their corresponding particle size distribution of AgNPs at different time are presented in Figure 7 (c) and (d). Sample A4, A5 and A3 have mean particles size of 4.39 nm, 88.97 nm and 54.66 nm, respectively. Sample A5 has shown the largest particles size decahedron shape. In comparison with TEM and particle size distribution, A4 resulted in small size and widely dispersed AgNPs while A5 and A3 produced bigger particle sizes.

4.3.1.3 Influence of pH on the formation of silver nanoparticles

The last parameter that was varied was pH to assess its influence on AgNP formation. The PVP solution was adjusted to pH 6, 9 and 10.5 as indicated in Table 3 for samples A6, A3 and A7. After adjusting the pH of PVP, silver nitrate solution was added and the solution was exposed to light for 3 h. Different colour changes were observed when varying pH. UV-Vis and TEM were used to characterise samples A6, A3 and A7 as shown in figure 8 and 9, respectively.

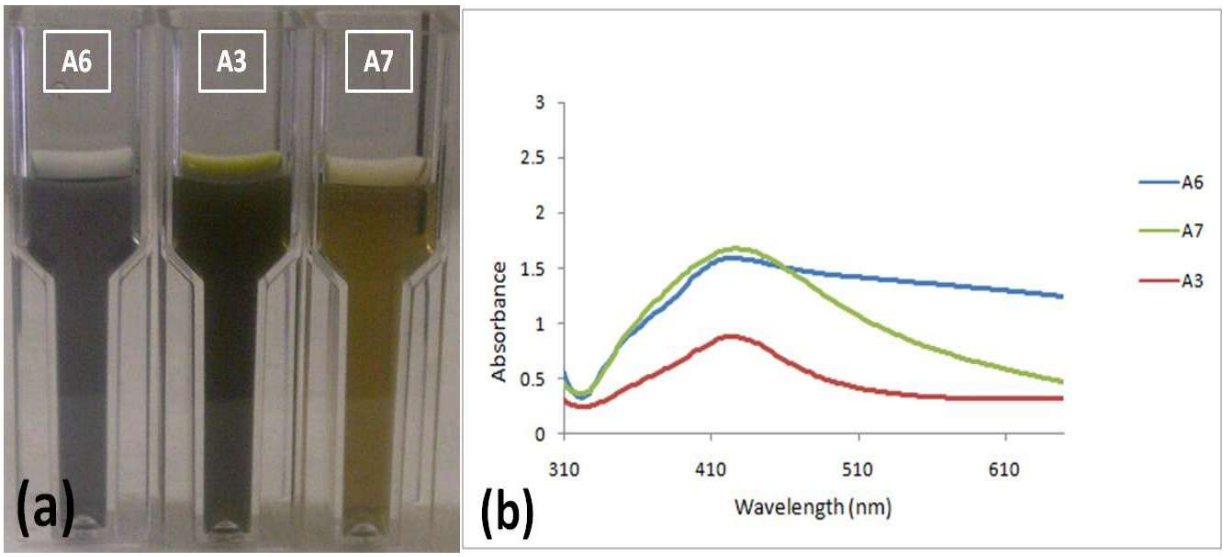

Figure 8: Synthesis of AgNPs at three different pH values. (a): Observable colour change at the different pH values 6, 9 and 10.5. (b): Corresponding UV-Vis absorbance spectra for A6, A3 and A7.

The colour change in Figure 8 (a) was observed after exposing silver nitrate and PVP solution to light with an adjusted pH of 6, 9 and 10.5 for A6, A3 and A7, respectively. The colourless solution of silver nitrate and PVP changed to gray, deep green and yellow (A6, A3 and A7) respectively. The change in colour is the initial indication of the formation of AgNPs.

The UV-Vis absorption spectrum was further used to confirm the formation of AgNPs as shown in Figure 8 (b). The pH adjustment to 6 (A6), which is known as circum neutral pH gave an absorbance band at 420 nm, indicating suppression of large nanoparticle formation. The alkaline pH of 9 (A3) and 10.5 (A7) showed a well-defined surface plasmon band centered at around 430 nm, which clearly indicated the synthesis of nanoparticles. The observations showed that by increasing the pH from neutral to alkalinity the absorbance band has red shifted from 420 nm to 430 nm indicating big particles sizes. Using photolight as a reducing agent, the low pH of 6 (A6) produced a shoulder band shifting to the shorter wavelength with very small nanoparticles, while high pH of 9 and 10.5 produced well defined AgNPs UV spectrums with larger sized nanoparticles. High pH level produces large number of nanoparticles with a smaller surface area (Vanaja *et al.,* 2013; Qin *et al*., 2010). The pH is considered as one of the factors that influence the synthesis of nanoparticles, as the size and the shape of nanoparticles are dependent on the pH of the solution (Vanaja *et al.,* 2013). The observations showed that sample A6 (circum neutral pH) produces the best AgNPs compared to alkaline pH (pH 9 and 10.5).

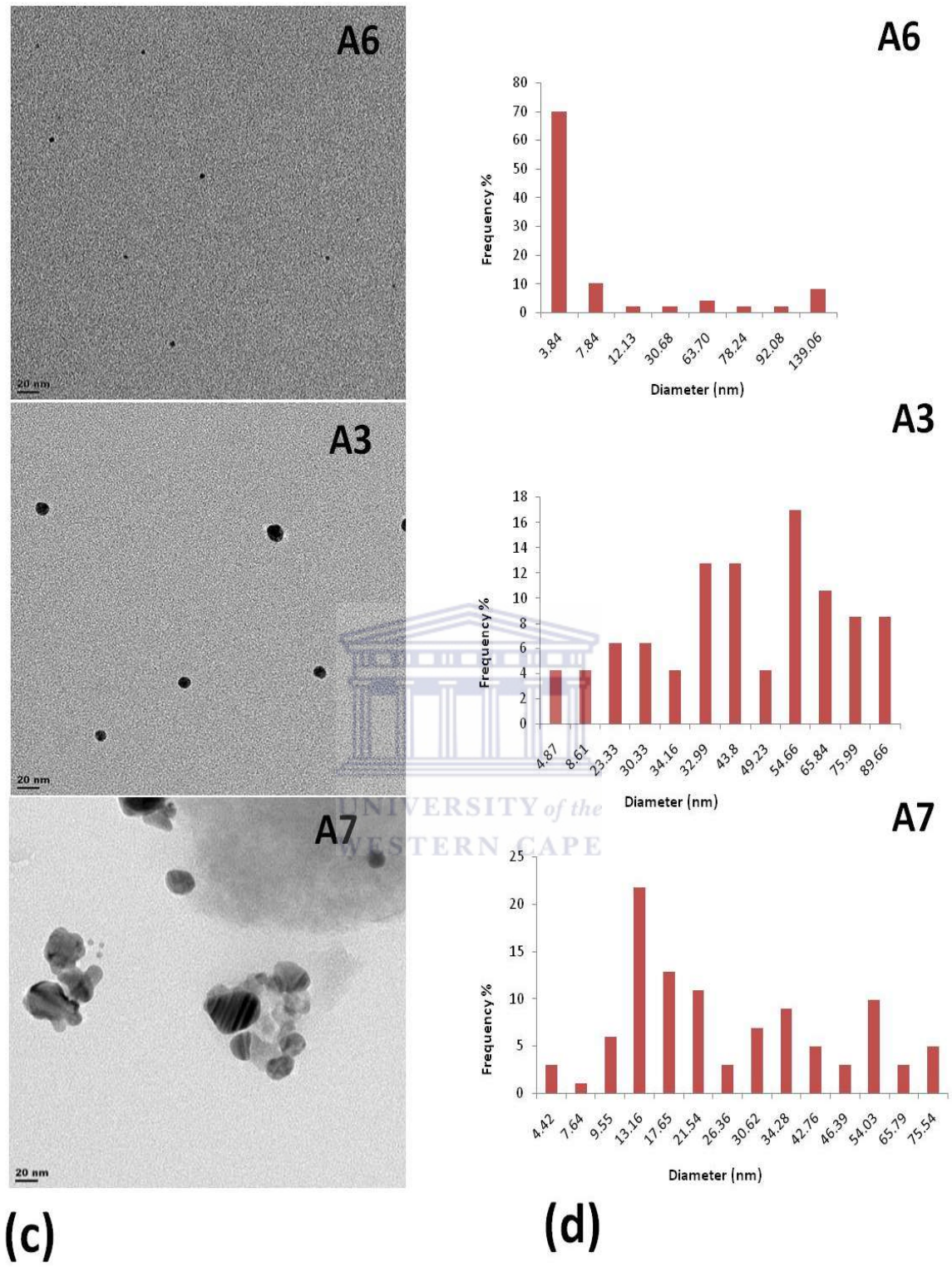

Figure 9: TEM analysis of AgNPs formed at different pH values. (c): TEM images and (d): size distribution of silver nanoparticles in A6, A3 and A7.

For further characterization of the results obtained in Figure 8 (b), TEM analysis was used to determine the size and morphology of AgNPs, as shown in Figure 9 (c). TEM images showed that in the case of A6 the particles are spherical in shape and very uniform in size and smaller than 7nm. The particle size distributions are shown in Figure 9 (d), where sample A6 has an average particle size of 3.48 nm, A3 and A7 have average particles size of 54.66 nm and 13.16 nm, respectively. Using the photolight synthesis, the observations in Figure 9 (d) shows that increase in pH increases the size of AgNPs.

4.3.2 Silver nanoparticles prepared in the presence of citric acid.

Silver nanoparticles were synthesized with citric acid as dispersant as described in section 4.2 Table 3. The following parameters were varied systematically: molar ratio of dispersant, exposure time to light and pH of citric acid. The samples were exposed to the light for 1, 2 or 3 h and pH was set at 9 and then varied to 6 and 10.5 (Table 3). UV-Vis analysis was used to determine the size and shape of nanoparticles formed and TEM was used to confirm the size and corresponding particle size distribution of the particles. Please note AgNPs colour change and UV-Vis figures are labelled (a) and (b) while TEM images and particle size distribution figures are labelled (c) and (d) respectively.

4.3.2.1 Influence of citric acid concentration on AgNPs formation

Samples B1, B2 and B3 (Figure 10 (a)), were obtained from three different concentrations of citric acid: 0.4, 2 and 4 mg/mL at the same pH. The citric acid solutions were added separately to silver nitrate solution and exposed to photolight for 3 h per sample. UV-Vis and TEM analysis were used to analyse samples (Figure 10).

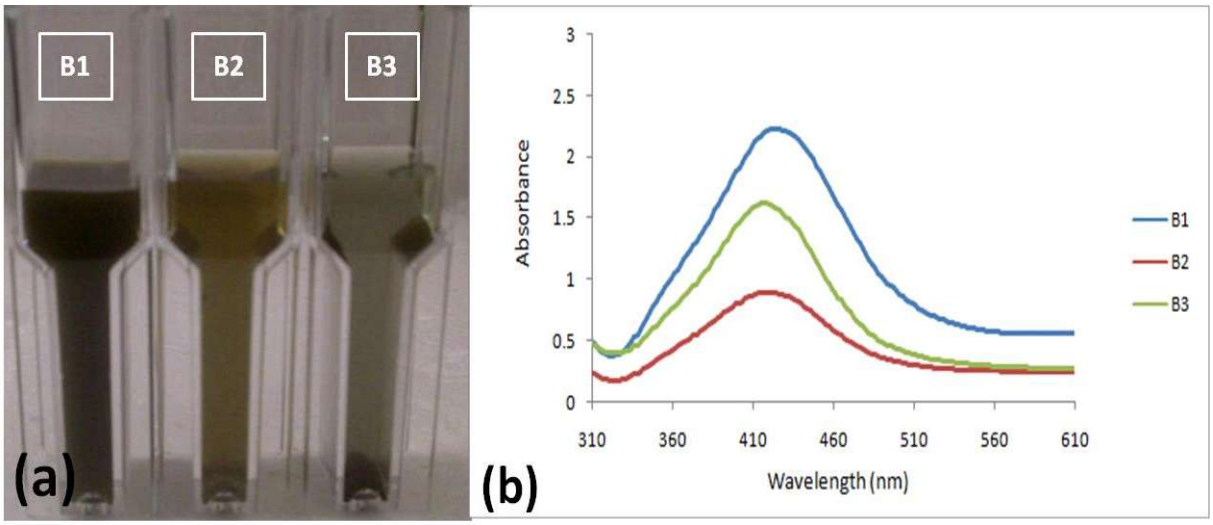

Figure 10: Colour change and UV-Vis analysis of citric acid formed AgNPs. (a): observable colour change at different citric acid concentration; B1, B2 and B3 = 0.4, 2 and 4 mg/mL citric acid respectively. (b): UV-Vis absorbance spectra of B1, B2 and B3 represented respectively by blue, red and green curves.

Figure 10 (a), showed the colour change of the solution at different concentrations of citric acid with silver nitrate reduced by light. The colourless citric acid/silver nitrate solution gradually turns brownish (B1), light brown (B2) and gray (B3) in 0.4, 2 and 4 mg/mL citric acid respectively. The colour change indicated the initial formation of AgNPs and it was confirmed by UV-vis (Figure 10 b) and TEM analysis (Figure 11).

UV-Vis both confirmed the formation of AgNPs and estimated their sizes and shapes. Sample B1 with a molar ratio of 0.4 to 0.4 of $AgNO_3$ to citric acid, showed an absorbance band at a wavelength around 430 nm, an absorbance of averagely large nanoparticles. As the molar ratio of citric acid to $AgNO_3$ increased to 2:0.2 (B2), and 4:0.2 (B3), the absorbance band wavelength decreased from 430 nm to 420 and 412 nm respectively. This is a precise indication that the higher the citric acid concentration the smaller and smoother the nanoparticles become. The sizes of these particles were further verified using TEM analysis (Figure 11).

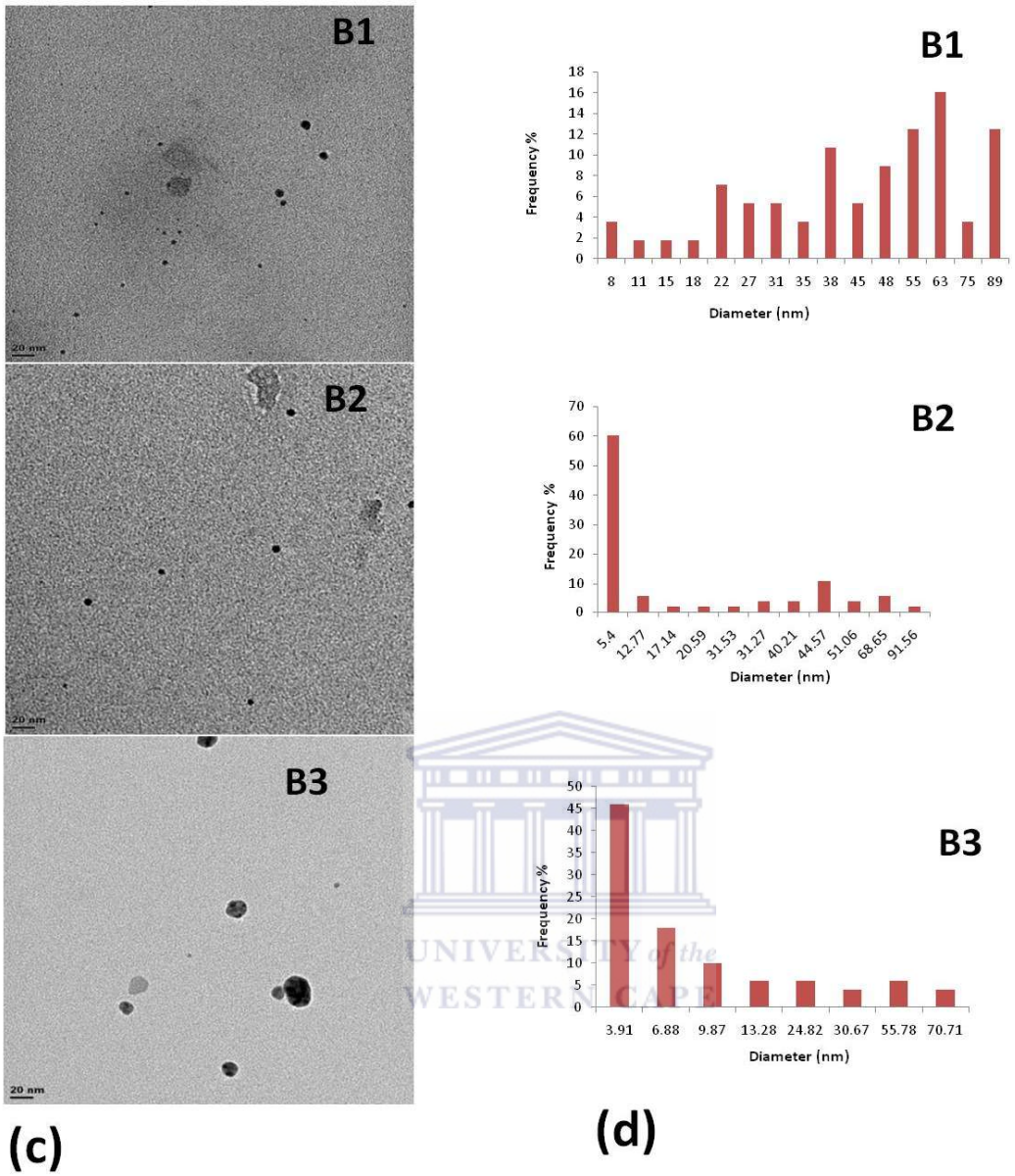

Figure 11: TEM analysis of AgNPs formed in different concentrations (0.4, 2 and 4 mg/mL) citric acid. (c): TEM images of B1, B2 and B3. (d): size distribution of silver nanoparticles in B1, B2 and B3.

TEM images in Figure 11 (c) showed that the nanoparticles were mainly of spherical shapes but of different sizes as expected for the three different concentrations of citric acid concentrations B1, B2 and B3. Though visual observation of the images (c) may suggest that B3 has the largest sizes, the size distribution analysis actually suggest as expected that B3 has the smallest particles sizes. Figure 11 (d) represents the particle size distribution of AgNPs, where sample B1 had a mean particle size of 63 nm. Sample B2 and B3 had a mean particle

size of 5.4 and 3.91 nm, respectively. Though visual observation of the images in Figure 11 (c) may suggest contrarily, namely that B3 has the largest sizes, the particle size distribution results in Figure 11 (d) confirms as expected that B3 has the smallest particles. This size distribution results correspond perfectly with the UV-Vis analysis (Figure 11 (c)) as the UV-Vis absorbance reading for B1, B2 and B3 blue-shifted from 430 nm to 420 nm and to 412 nm indicating a corresponding decrease in particle sizes**.** These results clearly suggest that the concentration of the dispersing agent citric acid is inversely proportional to the sizes of AgNPs formed in a$AgNO_3$/citric acid reaction at constant pH.

4.3.2.2 Influence of the time of light exposure on the formation of AgNPs.

Energy is transferred in the form of photons of light and the number of photons that interact with a sample may have a large effect on the outcome of the reaction. In this analysis, the effect of exposing light on the formation of AgNPs was verified by exposing three different samples B4, B5 and B3 to the same light source for different duration of time namely 1, 2 and 3 hours (Section 4.2). The effects of the exposure of the same concentration of silver ions and citric acid solution in B4, B5 and B3 to light for 1, 2 or 3 h, respectively were monitored first by observing the visual colour difference, and then analysing by UV-vis and TEM. A visual colour change to a light green, gray and brown solution was observed for the respective exposure times (Figure 12 (a). Figure 12 (b) shows a UV-vis spectrum of the samples and Figure 13 shows a TEM analysis of the sample.

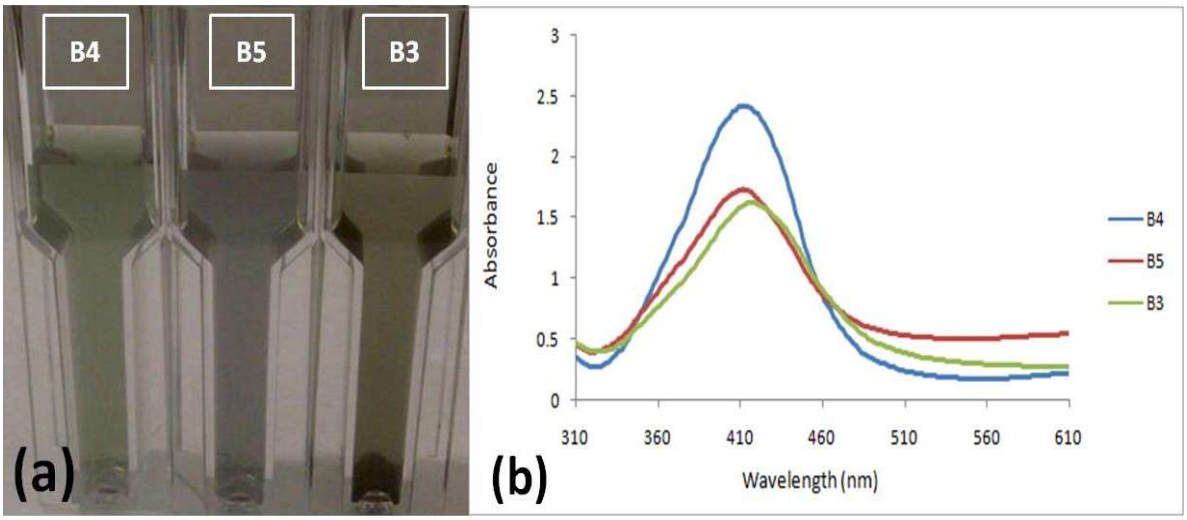

Figure 12: Visual colour observation and UV-vis analysis of the effect of light exposure time on AgNPs formation. (a): Colour change from light green (B4), to gray (B5) and brow (B3). (b): UV-vis absorbance spectrum of B4, B5 and B3.

Figure 12 (a) shows the first indication of the formation of AgNPs, a colour change from the colourless citric acid/$AgNO_3$ solution to light green, gray and brown solutions as a result of exposure to the same amount of light at different durations of time. The observations suggest a definite effect of amount of light on the formation of AgNPs. The spectrum shows that B4 absorbs at highest wavelength of about 420 nm, B5 at about 412 nm and B3 at about 415 nm. This changes in wavelength suggest that largest size nanoparticles were formed after 1 h and that further exposure to light refines the particles to smaller sizes but and over exposure to light starts causing the particles to increase in size again. Hence an optimized amount of light is needed to obtain AgNPs of a particular size. UV-vis absorbance spectrum of the samples shows that the particles absorb the greatest amount of light after exposure to light for an hour (420 nm in B4). Further exposure, however, results in a decrease in the wavelength of length of light absorbed (412 nm in B5 after 2 h). Counter intuitively, further exposure rather changes the absorbance wavelength to the increasing direction from 412 nm in B5 after 2 hours to 415 nm after 3 hours in B3. When correlating nanoparticles absorbance wavelength to particle size distribution it shows that the largest particles are formed

immediately at the beginning of reaction exposure to light. These particles decrease in size to optimum particle size at a particular light energy absorbance after which the particles start deforming and increasing in size again. This preposition was verified by TEM as recorded in Figure 13

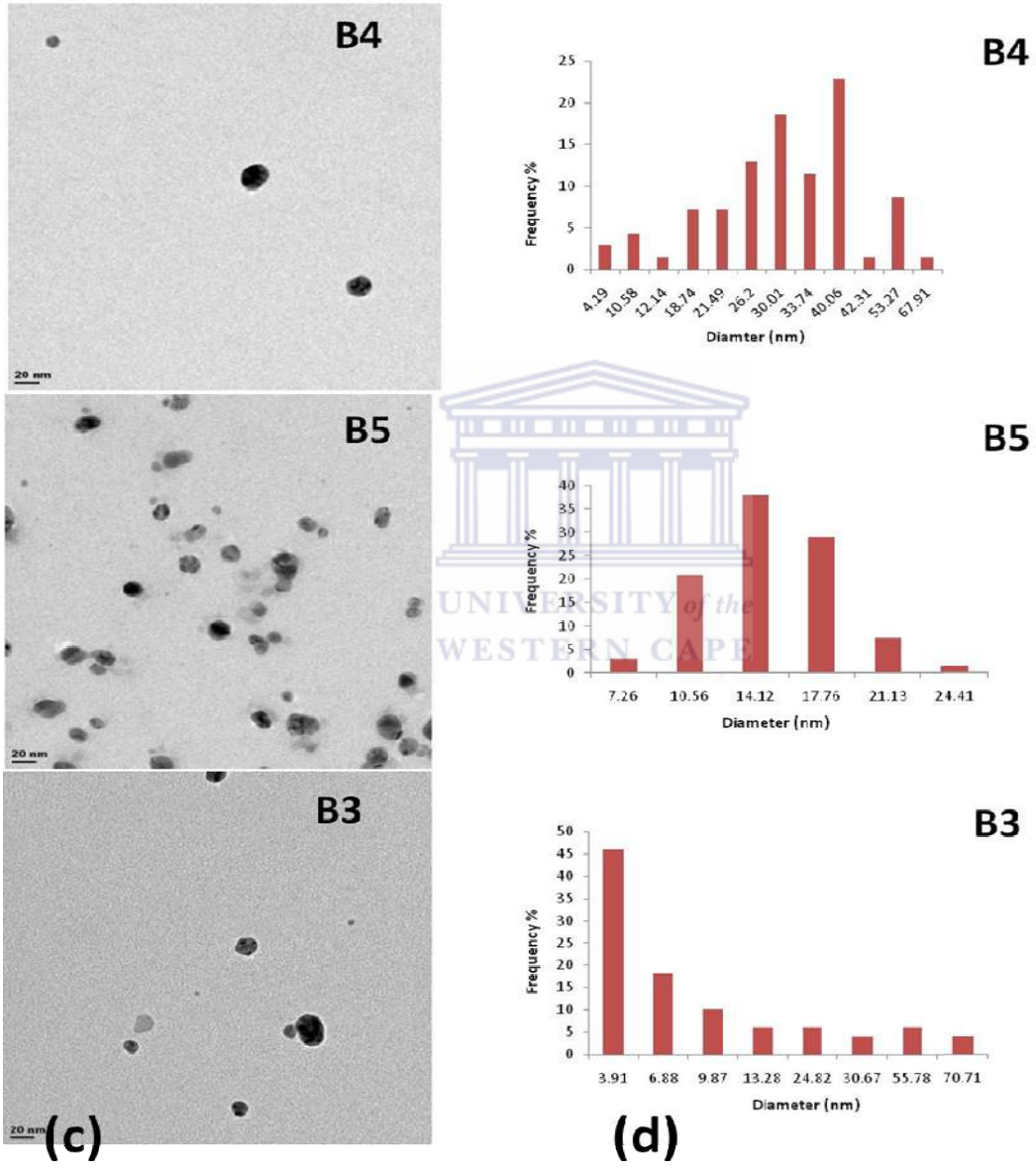

Figure 13: TEM image analysis and particle size distribution of AgNPs formed from exposure of citric acid/$AgNO_3$ solution to light for 1 hour (B4), 2 hour (B5) and 3 hours (B3). (c): TEM images of B4, B5 and B3 adjusted to a 20 nm scale; (d): size distribution of silver nanoparticles in B4, B5 and B3.

TEM images presented in Figure 13 (c) showed spherically shaped AgNPs in all samples (B4, B5 and B3) and nanoparticles were highly distributed in B4 and B3, while B5 showed slightly agglomeration of AgNPs. The images (c) show sparsely distributed spherical particles in B4 and B5 but slightly agglomerated particles in B3. The average size distribution (d) indicates that the particle sizes decreased with an increase in exposure time. This is not directly in agreement with the UV-vis observation that there is an initial decrease of particle size with exposure time, which started to increase after a certain light exposure. The images are in line with the UV-vis observations in Figure 12 as there is a clear indication that the particle sizes at the beginning of light exposure are larger in size compared to those obtained after two hours of light exposure. It can be seen that 2 h exposure time was the optimum exposure time as there are a good number of particles formed and of small sizes. Agglomeration of the particles at this time suggest that too many have formed and potentially calls for the adjustment of the reactant concentrations or the solution's pH. Further exposure at 3 h shows disappearance and increase in size of the particles, an observation that correlates once again with the UV-vis observation and which, therefore calls one to, always be precise with the amount of light and time of exposure when nanoparticles of a particular size and quantity are desired. Readings from the size distribution plots of Figure 13 (d) agree perfectly with the observation in the Figure 13 (c) image of B4 and B5 showing a mean particle size of 40.06 nm in B4 and 14.12 nm in B5. However, there is a sharp disagreement between the observation in B5 and B3 where UV-vis and TEM images suggest a reverse in observation i.e. an increase in particle sizes from B5 to B3. The mean particle size according to the plot in Figure 13 (c) further decreases from 14.12 nm to 3.91 nm. This abnormality may be attributed to the disrupted, irregular and changing structures of the particles as experimental time proceeds. However, this observation calls for further verification.

4.3.2.3 Effect of pH on the formation of AgNPs

The pH of a solution is the measure of the hydrogen ion or hydronium ion content of the solution. pH effects reactions in very different ways. In this section, the effect of pH on the formation of AgNPs using citric acid and $AgNO_3$ was investigated. The citric acid solution was adjusted using 3 M NaOH to pH 6, 9 or 10.5 for samples B6, B3 and B7 (Table 3). The same concentration of citric acid was added to each of the citric acid solutions in B6, B3 and B7 and the solution exposed to light for 3 h. Like in previous sections, colour change was monitored as indication of AgNPs formation and UV-vis and TEM analysis were used to investigate the sizes and shapes of the particles. Figures 14 and 15 document the outcomes of these investigations.

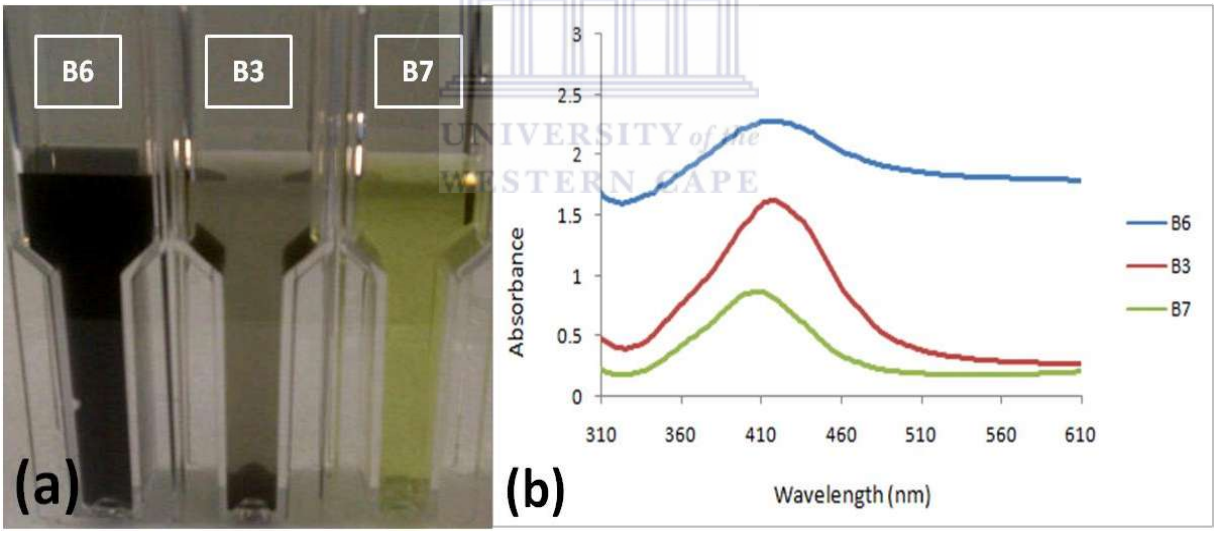

Figure 14: Verification of the formation of AgNPs at three different pH values. (a): Colour change observations after 3 h in pH 6, 9 and 10.5 in B6, B3 and B7.

As expected, pH variations definitely influenced the formation of AgNPs. The colour changes, from the colourless citric acid/$AgNO_3$ solution to black in B6, gray in B3 and yellow in B7 after 3 h of exposure to light. (b) UV-Vis absorbance spectrum of the AgNPs formed in B6, B3 and B7. The spectrum shows that B7 and B3 absorb UV-radiation of the

same wavelength, 413 nm although B6 also shows a broader spectrum curve. B7 for its part, showed the absorbance of a slightly shorter wavelength at 410 nm. Hence higher pH values favoured formation of smaller and well defined AgNPs. It was observed that increasing the pH from weak acid point at pH 6 to a strong basic point at 9 and 10.5 resulted in the fine tuning of the broad spectrum curve observed for B6 (pH 6) to a narrower symmetrical curve for B3 and B7 at pH 9 and 10.5 respectively. B6 and B3, though different in the broadness and symmetry of the absorbance curve, do absorb UV of the same wavelength 413 nm, indicating that there is no significant difference between AgNPs formed at pH 6 and pH9. The narrower and more symmetrical spectral curves of B3 and B7, however indicate that more well-defined and smooth particles are formed at these higher pH values. Also there is a slight shift in the UV absorbance at pH 10.5 to 410 nm indicating that the particles are not only well defined but are also smaller in size. The results suggest that pH values above 9 are good for AgNPs formation. These observations were further verified by TEM analysis as recorded in Figure 15.

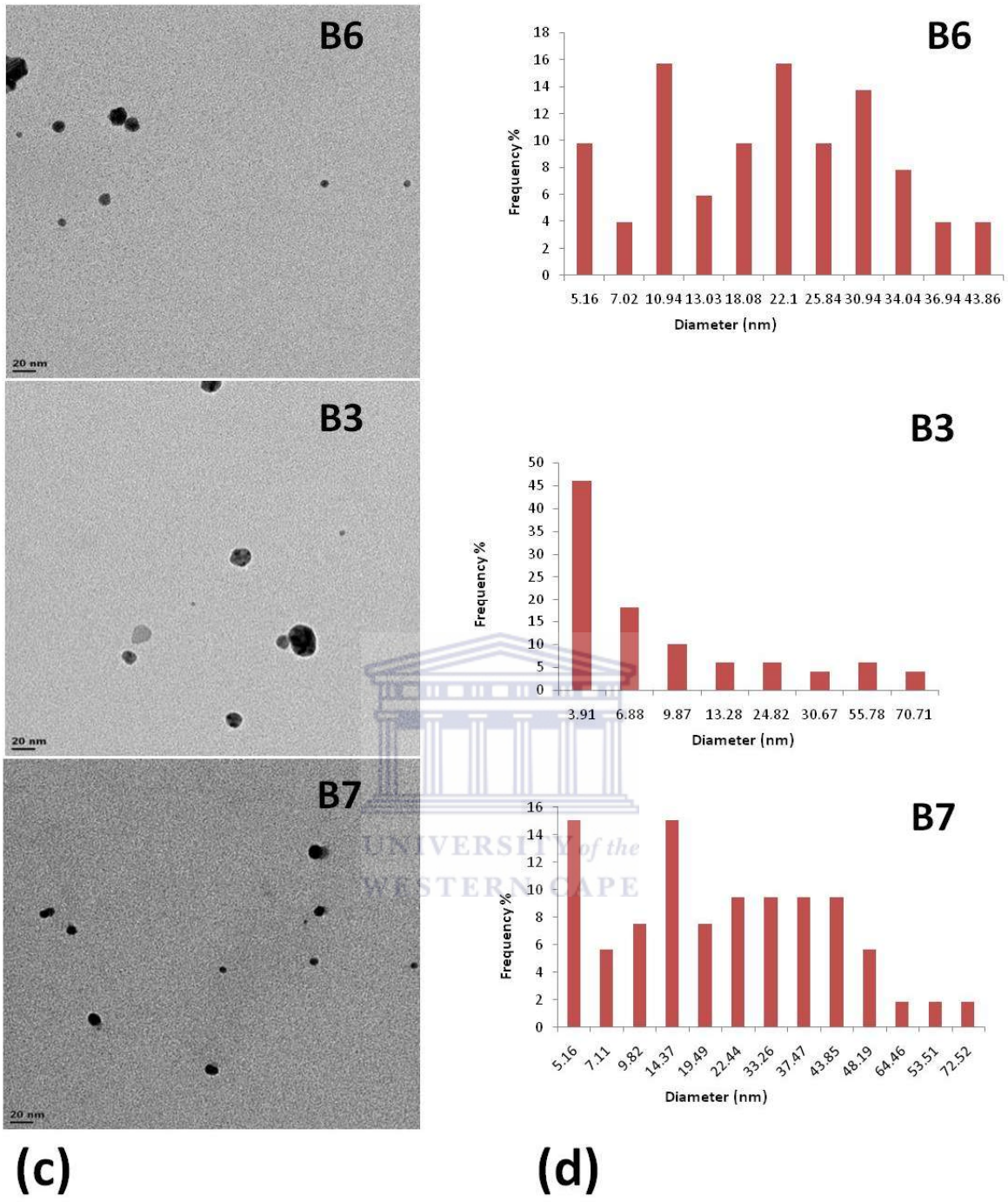

Figure 15: TEM images and size distribution of AgNPs formed at pH 6, 9 and 10.5 after 3 h of exposure to light. (c): TEM images of samples from B6, B3 and B7; (d) size distribution plots of the corresponding TEM images B6, B3, B7.

The TEM images presented in Figure 15 (c) show that the particles obtained are spherical in shape, with sizes in the 100 nm range. The TEM images and their size distribution also reveal that, the mean diameter of B6 was 10.9 nm, B3 was 3.91 nm and B7 was between 5.16 nm

and 48.19 nm. The results here do not agree with the suggestion of the UV-vis observations namely, B7 and B3 absorbed UV at the same wavelength hence, potentially have particles of the same size, and B7 absorbs at a lower wavelength of 410 nm hence, smaller size particles.

The inconsistency and non-correlation between UV-vis suggestion and TEM size distribution calls for a further investigation of the experiments and their application in preparing of nanoparticles. Nonetheless, these instruments were used to confirm the formation of AgNPs and to individually characterize them. These particles would be used in the next section of this work to investigate their toxicity on the eukaryotic unicellular yeast, *S. cerevisiae,* as a model to postulate the effect of the particles on eukaryotes cells in general.

References 2

1. Huang, H. H.,Ni, X. P., Loy, G. L., Chew, C. H., Tan, K. L., Loh, F. C., Deng, J. F. and Xu, G. Q. Photochemical formation of silver nanoparticles in poly (N-vinylpyrrolidone). *Langmuir*, (1996); **12**:909-912.
2. Qin, Y., Ji, X., Jing, J., Liu, H., Wu, H. and Yang W. Size control over spherical silver nanoparticles by ascorbic acid reduction. *Colloids and Surfaces A: Physicochemical Engineering Aspects.* (2010); ***372*:** 172–176.
3. Shameli, K., Ahmad, M. B., Jazayeri, S. D., Shabanzadeh, P., Sangpour, P., Jahangirian, H. and Gharayebi, Y. Investigation of antibacterial properties silver nanoparticles prepared via green method. *Chemistry Central Journal*, (2012); **6**:73.
4. Vanaja, M., Gnanajobitha, G., Paulkumar, K., Rajeshkumar, S., Malarkodi, C. and Annadurai, G. Phytosynthesis of silver nanoparticles by *Cissus quadrangularis*: influence of physicochemical factors. *Journal of Nanostructure in Chemistry*, (2013); **3**:17.
5. Brause, R., Moeltgen, H. and Kleinermanns, K. Characterization of laser ablated and chemically reduced silver colloids in aqueous solution by UV/VIS spectroscopy and STM/SEM microscopy. *Applied Physics B*. (2002); **75**:711-716.

CHAPTER 5

The assessment of toxicity of silver nanoparticles using *Saccharomyces cerevisiae* as bio-indicator.

Abstract

Silver nanoparticles (AgNPs) are commonly used in consumer products to prevent the undesirable growth of bacteria, fungi and algae. The release of these nanoparticles from consumer and household products into waste-water streams and further into the environment may pose a threat to non-target organisms, such as natural microbes and aquatic organisms. The aim of this study was to investigate the toxicity of AgNPs using the yeast, *Saccharomyces cerevisiae* (*S. cerevisiae)*. The toxicity of AgNPs was assessed using cell metabolic activity as biomarker. Metabolic activity was monitored using XTT chromogenic assays. *S. cerevisiae* was incubated with Malt Extract Broth (MEB) containing different concentrations of AgNPs at 37^{o}C for 24 h. After the incubation, XTT assays were performed to assess the cell proliferation. The XTT results showed that high concentration of AgNPs inhibit the growth of *S. cerevisiae*. The data obtained also showed that different methods applied in synthesizing AgNPs results to particles with different toxicity potentials. Data also showed that the degree of toxicity is dependent on the shape and size of the nanoparticles.

Keywords: AgNPs, toxicity, *S. cerevisiae,* XTT assay

5.1 Introduction

The distinctive chemical and physical properties of silver nanoparticles make them excellent candidates for antimicrobial activity (Jun Sung, *et al*., 2007). In addition, their antimicrobial and anti-inflammatory properties also make them good candidates for many purposes in the medical field (Panyala *et al*., 2008). However, the release of silver nanoparticles into the environment is a potential thread to both aquatic and non-aquatic life (Reidy *et al*., 2013). Studies and reports suggest that silver nanoparticles cause adverse effects in humans (Prabhu and Poulose, 2012). It is estimated that tonnes of silver nanoparticles are released from industrial wastes and it is believed that the toxicity of silver in the environment is due to free silver ions in the aqueous phase. The effect of free silver ions on human and animals, when ingested include permanent bluish-gray colouration of the eyes or the skin (Panyala *et al*., 2008). Exposure to soluble silver nanoparticles may lead to kidney and liver damage, and to changes in the morphologies of blood cells.

Hassain *et al*., (2005) assessed the *in vitro* toxicity of several nanoparticles, including silver nanoparticles (15 and 100 nm) on a rat liver derived cell line (BRL 3A).After 24 h of exposure, the mitochondrial function and membrane integrity (measured as Lactose Dehydrogenase (LDH) leakage) were significantly decreased. The LDH leakage was a result of the dose of AgNPs and was more severe for 100 nm than 15 nm particles. Evaluation with visual microscopy indicated that not all nanoparticles accumulated in the cell, some remained associated with membranes. All tested nanoparticles (Fe_3O_4, Al, MoO_3, and MnO_2) appeared to be less toxic than AgNPs. The observed cytotoxicity was due to oxidative stress, as indicated by the detection of intracellular glutathione (GSH) depletion, reduced potential of mitochondrial membrane and increased ROS levels (Hussain *et al*., 2005). Similar concentration-dependent cytotoxicity was observed when the same AgNPs were introduced on a mouse cell line, with spermatogonial stem cell characteristics under study (Braydich-

Stolle *et al*., 2005). In another study, AgNPs (~30 nm) were again classified amongst the most cytotoxic nanoparticles compared to TiO_2, Fe_2O_3, Al_2O_3, ZrO_2 and Si_3N_4. These particles were tested on marine alveolar macrophage cell line, human alveolar macrophage cell line and epithelial lung cell line (Soto *et al.,* 2005, 2007). Silver nanoparticles aggregates are said to be more toxic than asbestos used for house roofing (Hussain *et al*., 2005). By using human alveolar epithelia cell line (A549), metallic nanoparticles (Ag, TiO_2, Ni, Zn and Al) were shown to induce variable levels of cellular toxicity in a dose dependent manner. In addition, neuroendocrine cells were found to be sensitive to the cytotoxic activity of silver nanoparticles (15 nm) (Hussain *et al*., 2005). Table 4 summarises the impact of AgNPs on various cell lines (Reidy *et al.,* 2013).

Table 4: Silver nanoparticles used in *in vitro* biological experiments and their impacts (Reidy *et al.*, 2013).

Study	Shape	Size (nm)	Coating	IC50	Organism	Main outcomes
Arora *et al* ., 2009	spherical	7–20	Not stated	61 µg/mL (fibroblasts) and 449 µg/mL (liver cel l)	primary fibroblasts and primary liver cells from Swiss albino mice	• Silver nanoparticles present in mitochondria and cytoplasm • Silver nanoparticles trigger cellular antioxidant mechanism
Braydich Stolle *et al* ., 2010	spherical	10, 15, 25 –30, 80 nm	Hydrocarbon, polysac charide	Not provided	mouse spermatogonial stem cells	• Size and coating dependent decline in cells proliferation at concentrations • =10 µg/mL (via disruption of GDNF/Fyn kinase signalling) • ROS production and/or apoptosis did not seem to play a major role • Particle coating was degraded upon interaction with the Intracellular
Trickler *et al* ., 2010	Spherical	28.3 ± 9.6, 47.5 ± 5.6, 102.2 ± 32.8	PVP	Not assessed (above concentrations used)	primary rat brain microvessel endothelial cells (rBMEC)	• Small -sized nanoparticles (10 –25 nm) are more likely to promote apoptosis or the production of ROS • Cytotoxic - size -dependent • Pro -inflammatory responses (IL -1β, TNF α and PGE2 release) - size and • Blood -brain barrier permeability - size -dependent increase, probably • Correlated with increased immunotoxicity.
Bouwmeester *et al* ., 2011	spherical	20 ± 2, 34 ± 3, 61 ± 5, 113 ± 8	Not stated	Not provided, but below concentrations studied (5 µg/mL)	Caco -2 and M - cells co -culture	• 6% –17% of the silver nanoparticles were dissolved to ions • The amount of silver ions that passed the Caco -2 cell barrier was eq ual for the silver ion and nanoparticle exposures • Silver nanoparticles caused changes in gene expression in a range of stress responses including oxidative stress, endoplasmatic stress response, and apoptosis • O bserved effects of the silver nanoparti cles are likely exerted by the silver ions that are released from the nanoparticles
Foldbjerg *et al* . 2011	Not stated	60 –70 (depending on method) 149 ± 37 in medium	Citrate, PVP, gum arabic	~5 µg/mL	A549	• Strong correlation between the levels of ROS and mitochondrial damage and • Early apoptosis • DNA damage induced by ROS

Colorimetric assays for cellular viability have been found to be suitable tools in the study of eukaryotic cell activity. A mainstay of such techniques is the use of tetrazolium salts, which have evolved since the description of the 3-(4, 5-dimethylthiazol-2-yl)-2, 5-diphenyltetrazolium bromide (MTT) assay (Kuhn *et al.,* 2003; Mosmann, 1983). The synthesis of 2,3-bis(2-methoxy-4-nitro-5-sulfophenyl)-5-[(phenylamino)carbonyl]-2H-tetrazolium hydroxide (XTT) has proved to be useful, since the water solubility of the formazan product enabled the simplification of assay performance. The MTT and XTT methods have been employed as assays for yeast viability due to their easy utilization (Kuhn *et al.,* 2003). The aim of this study was to evaluate the effects of various AgNPs on cell viability of *S. cerevisiae* using the XTT assay.

5.2 Materials and Methods

5.2.1 Agar preparation

Potato Detrose agar (PDA) (Sigma-Aldrich)was prepared by adding 500 ml of water into a bottle containing 19.5 g of PDA and homogenized by mixing. It was then sterilized in an autoclave at 121ºC for 20 min. Immediately after autoclaving, the agar was allowed to cool down to room temperature (tilting the bottle to avoid solidification). The agar was poured into sterile petri dishes and allowed to cool down until the agar solidified. The plates were then stored at 4 ^{o}C.

5.2.2 Medium preparation

Malt extract broth (MEB) (Thermo Scientific) was prepared by adding 500 ml of water into a bottle containing 10 g of MEB and the mixture homogenised. Thereafter, 100 ml of MEB was transferred into an Erlenmeyer flask and the rest of the broth was transferred into test tubes. The broth was then sterilized in an autoclave at 115ºC for 10 min. The autoclaved medium was cooled to room temperature. The 100 ml broth in an Erlenmeyer flask was used for the yeast inoculation and the test tubes were stored at 4 ^{o}C for further use.

5.2.3 XTT preparation

2,3-Bis(2-methyloxy-4-nitro-5-sulfophenyl)-5-[(phenylamino)carbonyl]-2H-tetrazolium hydroxide (XTT) assays was purchased from Roche diagnostic in South Africa. XTT together with its capping reagent were incubated at room temperature to thaw. One millilitre of XTT was transferred into 2 ml Eppendorf tube and 20 µl of capping reagent added. The reagents were mixed and were ready to be used in an experiment.

5.2.4 Preparation of yeast stock cultures

An autoclaved swab was dipped into instant baker's yeast containing viable *S. cerevisiae* cells and inoculated into 100 ml of sterile MEB in an Erlenmeyer flask. The broth was incubated overnight at 37^{o}C. Four PDA plates (labelled 1-4) were streaked with *S. cerevisiae* from the overnight culture and incubated overnight at 37^{o}C. *S. cerevisiae* colonies were then picked up from each incubated plate and streaked out into new PDA agar plates. The plates were incubated overnight at 37^{o}C. After that, a single colony was picked and inoculated into 30 ml of MEB and incubated for 24 h at 37^{o}C. After 24 h of incubation, the cells were transferred into 50 ml tubes and centrifuged for 5-10 min (ensuring that the yeast cells accumulated at the bottom of the tube). The supernatant was discarded and the yeast cell pellet was resuspended with 10 ml of sterile water and 50 % glycerol was added to prevent the cells from fracturing. The yeast stock was stored at 4 ^{o}C.

5.2.5 XTT assay

Yeast stock (100 µl) was added to 10 ml of MEB and incubated overnight at 37^{o}C. Doubling dilutions of AgNPs in 10 % MEB were prepared to give 1 ml of each of the following AgNP concentrations: 0.78, 1.56, 3.125, 6.25, 12.5, 25, 50 and 100 µg/ml. A negative control tube containing 0.1 % Sodium Dodecyl Sulfate (SDS) in 10 % MEB was also prepared. The yeast cells (100 µl) were added thereafter to all tubes, including controls. The tubes were incubated for 74 h at 37^{o}C. After the incubation and centrifugation, the supernatant was discarded and the pellet washed with 1000 µl sterilized water. The cell pellet was resuspended in 1 ml of distilled water after which 50 µl of the resuspended cells was transferred to a 96 well plate. Filtered water and 0.1% SDS solutions were also used as controls. The XTT solution (Section 5.2.3) was added in each well and the initial Optical Density (OD) readings were taken using a plate reader at 450 nm. The plate was incubated for 24 h at 37^{o}C and OD readings were

again recorded. The change in OD at 450 nm over the 24 h period was calculated and used to determine the percentage metabolic activity of the cells. The percentage metabolic activity was calculated using the formula:

Percentage metabolic activity = (Change in absorbance of the sample)/ (change in absorbance of the 0 µg/ml AgNP control) x 100**……Equation 1**

5.3 Results and Discussion

Synthesis of silver nanoparticles

In order to assess the toxicity of AgNPs to *S. cerevisiae,* AgNPs were synthesised according to the protocols described in chapter 4. The nanoparticles were then characterized using UV-Vis and TEM. The results of optimization of synthesis condition showed that pH, light exposure time, concentration and type of dispersing agents produce AgNPs of different sizes and shapes. The different AgNPs synthesized in this work were used in their crude form i.e. without purifying, to investigate the toxicity of AgNPs on *S. cerevisiae*.

Tables 4 (A1 to A7) and 5 (B1 to B7) summarize the protocol used to prepare AgNPs by changing three parameters: molar ratio, light exposure time and pH. They also summarize the TEM results in terms of their different shapes and sizes and particle size distribution.

Table 5: Silver nanoparticles preparation with PVP and their size and shape.

Sample ID	Silver nanoparticles preparation	Ratio AgNO3: PVP	pH	Shape	Particle size distribution (nm)
A1	0.4 mg/mL of PVP was adjusted to pH 9 using 1 M NH_4NO_3 and 1 M citric acid. 0.4 mg/mL of $AgNO_3$ was added into PVP solution. The mixture was then exposed to the light (OSRAM Vitalux lamp) for 3 h	01:01	9	Needle-like	39-170
A2	2 mg/mL of PVP was adjusted to pH 9 using 1 M NH_4NO_3 and 1 M citric acid. 0.4 mg/mL of $AgNO_3$ was added into PVP solution. The mixture was then exposed to the light (OSRAM Vitalux lamp) for 3 h	01:05	9	Spherical	5-14
A3	4 mg/mL of PVP was adjusted to pH 9 using 1 M NH_4NO_3 and 1 M citric acid. 0.4 mg/mL of $AgNO_3$ was added into PVP solution. The mixture was then exposed to the light (OSRAM Vitalux lamp) for 3 h	01:10	9	Spherical	33-66
A4	4 mg/mL of PVP was adjusted to pH 9 using 1 M NH_4NO_3 and 1 M citric acid. 0.4 mg/mL of $AgNO_3$ was added into PVP solution. The mixture was then exposed to the light (OSRAM Vitalux lamp) for 1 h	01:10	9	Spherical	5-13
A5	4 mg/mL of PVP was adjusted to pH 9 using 1 M NH_4NO_3 and 1 M citric acid. 0.4 mg/mL of $AgNO_3$ was added into PVP solution. The mixture was then exposed to the light (OSRAM Vitalux lamp) for 2 h	01:10	9	Decahedrons	40-89
A6	4 mg/mL of PVP was adjusted to pH 6 using 1 M NH_4NO_3 and 1 M citric acid. 0.4 mg/mL of $AgNO_3$ was added into PVP solution. The mixture was then exposed to the light (OSRAM Vitalux lamp) for 3 h	01:10	6	Spherical	4
A7	4 mg/mL of PVP was adjusted to pH 10.5 using 1 M NH_4NO_3 and 1 M citric acid. 0.4 mg/mL of $AgNO_3$ was added into PVP solution. The mixture was then exposed to the light (OSRAM Vitalux lamp) for 3 h	01:10	10.5	Spherical	13-22

Table 6: Preparation of silver nanoparticles with citric acid and their size and shape

	Silver nanoparticles preparation				
Sample ID	Description: Preparation of silver nanoparticles with citric acid	Ratio $AgNO_3$: PVP	pH	Shape	Particle size distribution (nm)
B1	0.4 mg/mL of citric was adjusted to pH 9 using 1 M NH_4NO_3 and 1 M citric acid. 0.4 mg/mL of $AgNO_3$ was added into citric acid solution. The mixture was then exposed to the light (OSRAM Vitalux lamp) for 3 h	01:01	9	Spherical	38-91
B2	2 mg/mL of citric was adjusted to pH 9 using 1 M NH_4NO_3 and 1 M citric acid. 0.4 mg/mL of $AgNO_3$ was added into citric acid solution. The mixture was then exposed to the light (OSRAM Vitalux lamp) for 3 h	01:05	9	Spherical	5
B3	4 mg/mL of citric was adjusted to pH 9 using 1 M NH_4NO_3 and 1 M citric acid. 0.4 mg/mL of $AgNO_3$ was added into citric acid solution. The mixture was then exposed to the light (OSRAM Vitalux lamp) for 3 h	01:10	9	Spherical	4-9
B4	4 mg/mL of citric was adjusted to pH 9 using 1 M NH_4NO_3 and 1 M citric acid. 0.4 mg/mL of $AgNO_3$ was added into citric acid solution. The mixture was then exposed to the light (OSRAM Vitalux lamp) for 1 h	01:10	9	Spherical	22-40
B5	4 mg/mL of citric was adjusted to pH 9 using 1 M NH_4NO_3 and 1 M citric acid. 0.4 mg/mL of $AgNO_3$ was added into citric acid solution. The mixture was then exposed to the light (OSRAM Vitalux lamp) for 2 h	01:10	9	Spherical	11-18
B6	4 mg/mL of citric was adjusted to pH 6 using 1 M NH_4NO_3 and 1 M citric acid. 0.4 mg/mL of $AgNO_3$ was added into citric acid solution. The mixture was then exposed to the light (OSRAM Vitalux lamp) for 3 h	01:10	6	Spherical	11-31
B7	4 mg/mL of citric was adjusted to pH 10.5 using 1 M NH_4NO_3 and 1 M citric acid. 0.4 mg/mL of $AgNO_3$ was added into citric acid solution. The mixture was then exposed to the light (OSRAM Vitalux lamp) for 3 h	01:10	10.5	Spherical	5-14

Table 7 (A1 to A7) and Table 8 (B1 to B7) show the outcomes of the AgNPs cytotoxicity assessed by XTT assay. The highlighted numbers are the most toxic concentrations of AgNPs to the *S. cerevisiae* cells and the un-highlighted ones are the non-toxic concentrations of AgNPs.

Table 7: Toxicity of AgNPs prepared using PVP as dispersing agent

Sample ID	%Survival	µg/ml AgNPs								
		Control	0.78125	1.5625	3.125	6.25	12.5	25	50	100
A1	Mean	100	102	103	101	102	99	27	20	17
	SD	4	4	6	4	2	2	2	0	1
A2	Mean	100	102	98	96	98	100	34	21	19
	SD	8	7	5	7	5	8	1	1	0
A3	Mean	100	101	101	105	104	104	101	72	20
	SD	3	3	3	4	3	4	5	26	1
A4	Mean	100	106	102	99	23	20	19	17	14
	SD	3	1	3	2	1	0	0	2	1
A5	Mean	100	106	105	106	53	24	22	21	18
	SD	3	2	2	2	2	0	1	2	2
A6	Mean	100	108	107	109	107	68	26	24	23
	SD	4	4	4	2	2	3	1	1	2
A7	Mean	100	99	99	90	23	13	12	10	8
	SD	5	2	2	3	3	3	1	1	1

Table 7 shows results of the toxicity of the synthesized AgNPs on *S. cerevisiae.* The results show clearly that higher concentrations of AgNPs are toxic to *S. cerevisiae* cells. At AgNPs concentrations above 6.25 µg/ml, the most toxic particles start their killing effect. And this assays shows A4, A5 and A7 to be the most toxic AgNPs in this series. Following that is A6, which kills at 12.5 µg/ml, and A1 and A2 that show toxicity at 25 µg/ml. the least toxic particles in this series A3 starts killing cells only at concentrations as high as 50 µg/ml. The cytotoxic data suggest that particles synthesise by different means demonstrate different toxicity levels on the cells. This means in synthesizing AgNPs for particular applications, the method of synthesis needs to be carefully investigated and optimised.

Table 8: Toxicity of AgNPs prepared using citric acid as dispersing agent

Sample ID	% Toxicity	µg/ml AgNPs								
		Control	0.78125	1.5625	3.125	6.25	12.5	25	50	100
B1	Mean	100	101	99	98	97	97	97	98	90
	SD	5	2	3	1	4	3	4	3	4
B2	Mean	100	112	114	115	114	100	103	100	29
	SD	4	8	5	3	4	2	11	25	1
B3	Mean	100	110	115	114	79	18	22	19	19
	SD	4	2	2	2	4	1	0	0	1
B4	Mean	100	112	109	103	116	109	20	21	20
	SD	2	1	2	16	2	3	0	1	1
B5	Mean	100	95	92	98	97	99	101	104	67
	SD	9	2	5	1	3	2	4	3	2
B6	Mean	100	96	95	99	98	99	98	93	27
	SD	5	1	1	4	1	1	3	1	1
B7	Mean	100	101	102	112	47	22	20	20	18
	SD	2	2	10	7	3	0	1	1	2

The results obtained in Table 8 showed no cytotoxicity in sample B1 while B2, B5 and B6 are cytotoxic to *S. cerevisiae* at concentration of AgNPs as high as 100 µg/ml. However, B4 starts showing cytotoxicity at concentrations above 12.5 µg/ml whilst B3 and B7 on the other hand, show cytotoxity from concentration of 6.25 µg/ml. The observations showed that different parameters used to prepare AgNPs differ in their cytotoxicity and cytotoxicity increased in the following order B1< B2; B5; B6 < B4< B3; B7. Comparatively, the A1-A7 series shows more cytotoxic effect on the *S. cerevisiae* cell than the B1-B7 series but both are cytotoxic at different concentration to the cells.

5.4 General Conclusion

The task of this research was to investigate the toxicity of silver nanoparticles (AgNPs) on *S. cerevisiae* cells as a model organism for eukaryotic cells. The results are to contribute to the knowledge required for the preparation of AgNPs water treatment strategy for poor communities. To accomplish this task, AgNPs were synthesized successfully by photochemical reduction of $AgNO_3$ in the presence of PVP and in the presence of citric acid. The formation of AgNPs was confirmed by UV-Vis absorption spectra analysis. The UV-Vis absorption spectra showed the Surface Plasmon Resonance (SPR) band characteristics of AgNPs in the range of 400-500 nm. TEM was also used to confirm the formation of AgNPs and to view their sizes and shapes and to verify the size distribution of the synthesised particles. TEM images showed that the AgNPs were in spherical, needle-like and decahendrons shape depending on the method of synthesis applied. The particles obtained using PVP were shown to be bigger in nano-size than those synthesized using citric acid (Table 5 and 6). The concentration of PVP and citric acid, time of light exposure and pH of reaction mixture affected the formation of AgNPs in unique ways.

Cytotoxicity of the synthesised AgNPs was evaluated using the XTT assay which assesses cell viability upon exposure to different concentrations of AgNPs. The assay showed that high concentrations of AgNPs (12.5, 25, 50 and 100 µg/mL) were toxic to the cell. The cell killing effect was greater with the PVP synthesised AgNPs than those from citric acid. It was also observed that the methods of preparation of the AgNPs influenced their toxicity. These observations were consisted with previous research on related topic (Braydich-Stolle *et al*., 2005, Carlson *et al.,* 2008) which showed that AgNPs are toxic to mammalian cells, and that the sizes of the particles influence their toxicity but contrary to their conclusion, this study showed that larger AgNPs are more toxic to *S. cerevisiae* than small particles. AgNPs

prepared and tested in this work were used in their crude form. Further investigation on this subject may consider purifying the AgNPs before proceeding to toxicity tests.

References 3

1. Braydich-Stolle, L., Hussain, S., Schlager, J.J. and Hofmann, M.C. *In vitro* cytotoxicity of nanoparticles in mammalian germlinestem cells. *Toxicological Science*.(2005); **88**:412-419
2. Carlson, C., Hussain, S. M., Schrand, A. M., Braydich-Stolle, L. K., Hess, K. L., Jones, R. L. and Schlager, J. J. Unique cellular interaction of silver nanoparticles: size-dependent generation of reactive oxygen species. *Journal of Physical Chemistry*. (2008); **112**:13608−13619.
3. Hussain, S. M., Hess, K. L., Gearhart, J. M, Geiss, K.T. and Schlager, J. J: In vitro toxicity of nanoparticles in BRL 3A rat liver cells. *Toxicology in vitro*. (2005); **19**: 975–983.
4. Jun Sung, K., Eunye, K., Kyeong, N.Y., Jong-Ho, K., Sung, J. P., Hu, J. L., So, H. K., Young, K. P., Yong, H. P., Cheol-Yong, H., Yong-Kwon K., Yoon-Sik, L., Dae, H. J and Myung-Haing, C. Antimicrobial effects of silver nanoparticles. *Nanomedicine: Nanotechnology, Biology, and Medicine*. (2007)**; 3**: 95– 101.
5. Kuhn, D. M., Balkis, M., Chandra, J., Mukherjee, P. K. and Ghannoum, M. A. Uses and limitations of the XTT assay in studies of *Candida* growth and metabolism. *Journal of Clinical Microbiology.* (2003); **41:** 506.
6. Kuhn, D. M., George, T., Chandra, J., Mukherjee, P. K. and Ghannoum, M. A. Antifungal susceptibility of *Candida biofilms*: unique efficacy of amphotericin B lipid formulations and echinocandins. *Antimicrob Agents Chemother* (2002); **46**:1773–1780.
7. Mosmann, T. Rapid colorimetric assay for cellular growth and survival: application to proliferation and cytotoxicity assays. *Journal of immunological Methods*. (1983); **65**: 55-63.

8. Panyala, N. R., Pena-Mendez, E. M. and Havel, J. Silver or silver nanoparticles: a hazardous threat to the environment and human health? *Journal of Applied Biomed*. (2008); **6**: 117–129.
9. Prabhu, S. and Poulose, E. K. Silver nanoparticles: mechanism of antimicrobial action, synthesis, medical applications, and toxicity effects. *Prabhu and Poulose International Nano Letters*. (2012**); 2:**1-1-10.
10. Reidy, B., Haase, A., Luch, A., Dawson K. A. and Lynch, I. Mechanisms of silver nanoparticle release, transformation and toxicity: A critical review of current knowledge and recommendations for future studies and applications. *Materials.* (2013); **6**: 2295-2350.
11. Soto, K., Garza, K. M. and Murr, L. E. Cytotoxic effects of aggregated nanomaterials. *Acta Biomater.* (2007); **3**:351-358.
12. Soto, K. F., Carrasco, A., Powell, T. G., Garza, K.M. and Murr, L. E. Comparative *in vitro* cytotoxicity assessment of some manufactured nanoparticulate materials characterized by transmission electron microscopy. *Journal of Nanoparticle Research*. (2005); **7:**145-169.